X-514-68-458

NASA TM X-63431

# COMPARISON OF C-BAND, SECOR AND TRANET WITH A COLLOCATED LASER ON 10 TRACKS OF GEOS-2


JOHN H. BERBERT
HORACE C. PARKER





NOVEMBER 1968



GSFC
GODDARD SPACE FLIGHT CENTER
GREENBELT, MARYLAND

# COMPARISON OF C-BAND, SECOR, AND TRANET WITH A COLLOCATED LASER ON 10 TRACKS OF GEOS-2

John H. Berbert
(NASA) Principal Investigator
GEOS Observation Systems Intercomparison Investigation

Horace C. Parker
RCA Service Company

November 1968

Goddard Space Flight Center
Greenbelt, Maryland

## ABSTRACT

## COMPARISON OF C-BAND, SECOR, AND TRANET WITH A COLLOCATED LASER ON 10 TRACKS OF GEOS-2

As part of the GEOS Observation Systems Intercomparison Investigation, several of the geodetic satellite tracking systems used with GEOS-2, including a NASA Laser, an Army SECOR, and a Navy TRANET, were moved to the NASA Wallops Island station and located near the FPQ-6 and FPS-16 C-band radars there. Simultaneous tracking of GEOS-2 by all these systems was accomplished during April, May, and June, 1968, to enable comparisons of the tracking data freed from the effects of uncertainties in survey, in the gravity field, and in systems time synchronization. Reference orbits were determined from the laser data. Comparison of tracking data from the radio tracking systems with the laser reference orbits yielded residuals from which zero-set and timing biases were derived for each system. The preliminary results for the 10 passes reported here indicate, for the SECOR, a consistent unexplained negative zero-set bias averaging about 10.8 meters. The two C-band radars generally agree with the laser to within ±5 meters. The TRANET data have an average positive bias of about 16.6 centimeters per second, which has been mostly explained by a procedure peculiar to the preparation of GEOS (and ANNA) data for the Geodetic Satellite Data Service (GSDS). More definitve results are expected later, when optical data are added into the reductions and more passes are reduced.

TABLE OF CONTENTS

## SECTION 1
## MISSION



## SECTION 2
## COLLOCATED SYSTEMS

TABLE OF CONTENTS (Cont)

## SECTION 3
## DATA PROCESSING



## SECTION 4
## ERROR PROPAGATION STUDY

## SECTION 5
## CONCLUSIONS



## SECTION 6
## FUTURE PLANS



## APPENDICES

## LIST OF ILLUSTRATIONS



## LIST OF TABLES

# SECTION 1
# MISSION

## 1.1 GENERAL

The Wallops Island Collocation Experiment (WICE) was performed as part of the Observation System Intercomparison Investigation (OSII) of the Geodetic Satellite Program at the instigation and under the direction of the NASA OSII Principal Investigator. The objective of the OSII is to intercompare the major geodetic satellite observation systems and to evaluate their accuracies.

The following observation systems were collocated at Wallops Island:

- FPQ-6 radar
- FPS-16 radar
- SECOR ranging system
- TRANET doppler system
- Laser radar
- BC-4 and PTH-100 cameras

These systems were closely grouped in order to provide a basis (minimum error due to survey, timing, and gravity unknowns) for intercomparison of the data provided by each system. The laser is used as the reference system to provide reference short-arc orbits from which accurate ranges and somewhat less accurate angles and range rates were computed and compared with the measurements made by the other systems. WICE was conducted over a 3-month period, commencing April 1, 1968.

Wallops Island provided and operated the FPQ-6 and FPS-16 radars and provided data to Goddard in modified Calsat format. Wallops also provided and operated the BC-4 cameras. Goddard is processing the BC-4 data. Goddard provided and operated the laser and the PTH-100 camera and is processing the associated data. The Army Map Service provided and operated the SECOR and is processing its data. The Naval Air Systems Command provided and operated the TRANET and is processing these data.

## 1.2 SCHEDULING AND PREDICTIONS

The experiment goal was to obtain 30 nighttime and 30 daytime passes with all systems tracking simultaneously and with supporting tropospheric and ionospheric measurements. Except on weekends, each laser pass which met the following criteria was scheduled:

- Maximum elevation above $40^{\circ}$ for single passes or $35^{\circ}$ for adjacent passes
- Satellite sunlit during some part of the pass

The Goddard Space Flight Center (GSFC) Computation Division (CD) and the Mission and Trajectory Analysis Division (MTAD) generated station predictions, scheduling information, and laser drive tapes for the collocation experiment stations. From this information, suitable passes were selected by the authors. Requests for these were forwarded to the Wallops Island Project Coordinator, H. Stanley, who coordinated the Wallops Island operations with the GEOS Operations Control Center (GOCC) at Goddard. GOCC coordinated these requests with other GEOS project requirements and scheduled the spacecraft.

## 1.3 REFRACTION STUDY

Data were taken to enable comparison between ray tracings of the ionosphere and analytic corrections based on National Bureau of Standards (NBS) predictions, the 2-frequency ionospheric refraction correction for SECOR, and the 2- and 3-frequency ionospheric refraction corrections for TRANET doppler. The WICE TRANET doppler system digitally recorded all three frequencies and the equivalent frequencies from both the low- and high-frequency pairs. The tropospheric ray trace will be compared to the analytic based on ground measurements of the index of refraction. In order to support the refraction studies, measurements of pressure, temperature, and relative humidity were made at the FPQ-6 radar site within one-half hour of each scheduled pass. Balloon soundings of the troposphere, which provided an index of refraction as a function of height, were made within one to two hours of the pass. Ionosonde soundings of the ionosphere were made every 15 minutes. Satellite top-side soundings fell near the time of some of the WICE passes. The time and ground separations of these passes are being studied, and several of the passes will be selected for a separate, detailed refraction study.

## 1.4 SURVEY

The Field Facilities Branch of GSFC performed survey determinations of geodetic latitude and longitude on the North American datum of 1927 and height above mean sea level on the sea level datum of 1929 for each of the WICE tracking systems. The accuracy of the positions of the other WICE systems relative to the laser is estimated to be 10 centimeters or better. Details of the survey are given in Appendix A.

## 1.5 TIMING

All collocated systems were required to refer to the Wallops Station master clock as their time standard. The master clock consisted of a portable cesium (Ce) standard driving a time-of-day generator (TODG). The master clock was referenced to UTC time at the U.S. Naval Observatory (USNO) and maintained to an accuracy of within ±50 microseconds by making monthly trips to the USNO with the Ce standard. Signals from the master clock were transmitted over cable to the WICE stations and used for reference prior to each pass. Cable delays were measured by comparing time ticks at the input and output of the cables, using the portable Ce standard. The cable delays were remeasured about every 2 weeks.

Whenever the Ce standard was disconnected from the TODG for cable delay measurements or for trips to the USNO, the delay between the Ce standard and the TODG varied from its nominal value of 200 $\mu$sec by $\pm$ 100 $\mu$sec. The changes in this value were recorded for use by the participants.

## SECTION 2
## COLLOCATED SYSTEMS

### 2.1 INTRODUCTION

This section contains a brief description of each system and its associated data preprocessing, calibration, and timing.

### 2.2 LASER

The laser tracking system placed at Wallops Island was operated by the Optical Systems Branch (OSB) of Goddard. This system uses an intense, highly collimated, short-duration beam of light for illuminating the spacecraft being tracked. At the spacecraft, the beam is reflected back towards the ground station by an array of cube corner reflectors. The returning light is detected photoelectrically, and its time of flight is measured to yield the range data. The actual laser transmitter is mounted on a radar pedestal along with a Cassegranian telescope used for receiving the reflected laser beam. When the laser system is tracking, the transmitter is flashed at 1 pulse/sec. Each transmitter pulse starts a time-interval-measuring unit necessary for range measurement. During the pass, the mount, equipped with digital encoders, is directed toward the expected position of the spacecraft by a programmer fed with punched paper tape. By using a telescope, the operator can see the spacecraft and make corrections to keep it within the illuminating beam, which is only about 1.2 milliradians wide. Along with a range measurement, both the azimuth and elevation of the spacecraft are recorded from the position mount. The laser tracking system is probably unbiased to 0.15 meter in range, with a random noise component of about 1.2 meters, and can produce range rates through an orbital fit to the range data which are good to about 1 cm/sec. These estimates include all known error sources except the scaling error of 1 part in $10^6$ due to the uncertainty in the velocity of light, which affects all systems. The angular accuracy with this laser is estimated to be about 0.5 milliradian or better. See reference 5.

#### 2.2.1 LASER DATA PREPROCESSING

The OSB personnel were responsible for laser data preprocessing. The preprocessor program accomplishes the following functions:

- Converts the recorded time of observation to the time when the laser pulse was at the spacecraft.

- Computes the range to the satellite from the round-trip time interval values and calibration values.
- Corrects the measured elevation angle for refraction.
- Corrects the computed range for refraction.
- Edits the data based on a five-sigma rejection criterion.
- Reformats the acceptable data points into the required Geodetic Satellite Data Service (GSDS) format and outputs the data on a magnetic tape, with a density of 1 observation per second.

Preprocessing details are contained in reference 1 and reference 2. The authors received the WICE laser data from GSDS and conducted this intercomparison study with no additional preprocessing.

### 2.2.2 LASER SYSTEM CALIBRATION

For angle calibrations, a special boresight feature is incorporated in the collimating optics for the transmitted beam, which allows the laser transmitter to be aligned parallel to the opto-mechanical axis of the tracking pedestal. Boresighting is accomplished by firing the laser through a separately attached focusing lens onto a piece of aluminum foil in its focal plane. The reflex viewer, which forms the boresight function on the collimating optics, is then inserted in the optical path, and its cross-hairs are adjusted to coincide with the hole formed in the foil by the focused laser beam. With the focusing lens removed, the reflex viewer is directed along the laser beam and can be used to bring the laser optical axis parallel to the other optical systems on the tracking pedestal.

For range calibrations, the total delay in signal due to telescope optical path length and delay through the photomultiplier tube is measured over a geodimeter calibrated range (3274.98 meters at Wallops) before and after each pass. See reference 1.

### 2.2.3 LASER SYSTEM TIMING

The laser data control unit generates all the control signals for operation of the laser and receiver systems. In addition, the unit maintains system time with respect to an external time source such as WWV or, as in the case of WICE, to the Wallops station master clock. This is accomplished by setting the laser control

unit. A 1-MHz oscillator, acting as a secondary time standard, is counted to one pulse per second through phase shift and delay circuits for synchronization with the external timing standard. At WICE the laser 1-pps signal is synchronized to about $\pm 0.05$ millisecond prior to each pass with the master clock cable signals adjusted for a cable delay bias and the current delay between the Ce standard and the TODG. The 1-pps signal is then used as the on-time generated pulse throughout the entire data control unit and operates a binary coded decimal (BCD) time code generator whose output is displayed visually as well as recorded through the data select gates for correction with measured range. The rotation prism Q-switch cannot maintain exact synchronism with the on-time pulse, and therefore, the laser may fire from 8.5 to 11 milliseconds after the command time. An uncertainty of this magnitude in the time of observation is not compatible with the accuracy requirements, so a delay time interval counter was incorporated in the data control unit to accurately measure the time of firing with respect to on-time. This counter is started by the on-time and stopped by a signal from the laser beam sample unit, giving the absolute time at which the laser fires to within 100 microseconds. The output of the delay counter is stored and transferred to the data select gates in parallel with the range-time-interval measurement for recording. This value is used in the preprocesser to correct the data time tag.

### 2.2.4 LASER SYSTEM TRACKING CONSTRAINTS

The GSFC laser located at Wallops had the following tracking constraints:

- Nighttime at the station (sun $10^{\circ}$ below the horizon).
- Satellite maximum elevation angle above $30^{\circ}$.
- Satellite sunlit or lamp flashing for visual acquisition.
- One safety operator at laser station to make visual observation for low-flying aircraft.
- An operational surveillance radar to verify that there were no aircraft within a 14-nautical-mile range.

## 2.3 SECOR

The SECOR system was operated by the Army Map Service (AMS). It operates on the physical principle that a modulated radio frequency signal passing

through space will undergo a phase shift proportional to the distance traveled and to the modulated frequency. This change, due to the time and distance traveled, is translated into the range between the transmitting and receiving stations. Ionospheric refraction effects are decreased by using two coherent carriers in the down-link, 224.5-MHz and 449.0-MHz. These carriers are modulated by the same ranging sidetones that modulate the up-link carrier.

The choice of ranging modulation sidetones is affected by two opposing considerations. To avoid ambiguities in the range measurements, the half-wavelength of the modulation signal must equal or exceed the maximum range desired; thus, a long-range capability requires that the ranging wavelength be very long. For good resolution, however, a high frequency is required so that small increments of range can be measured. SECOR has four harmonically related modulation signals linearly combined into a phase modulation baseband. This provides a system resolution of 0.25 meter, eliminates range ambiguities, and provides a maximum unambiguous range capability of 7500 kilometers.

## 2.3.1 SECOR DATA PREPROCESSING

AMS personnel were responsible for secor data preprocessing. The preprocessor program accomplishes the following functions:

- Computes the time of observation, which is defined as the time when the pulse was at the spacecraft.
- Makes ambiguity corrections to the edited range measurements.
- Applies calibration values to the edited range measurements.
- Applies tropospheric refraction to the range measurements.
- Uses the difference between ranges measured on the low- and high-frequency carriers from the spacecraft to com[illegible] a correction for retardation due to the ionosphere. The range is corrected for this value, and the ionospheric correction value is included in the output.
- Reformats the data into the required GSDS format and outputs the data on a magnetic tape, with a density of 1 observation per 4 seconds.

The authors received the WICE SECOR data from GSDS and conducted intercomparison studies with no additional preprocessing.

### 2.3.2 SECOR SYSTEM CALIBRATION

In the calibrate mode, the calibration oscillator generates 196.4 MHz. This is fed to a mixer mounted above the vertical axis of the WICE station dual-reflector antenna system and between the up-link and down-link reflectors. A 420.9-MHz ground station up-link carrier frequency is radiated, from the up-link antenna to the mixer, to produce 224.5 MHz and its second harmonic, 449.0 MHz, which are the spacecraft down-link carrier frequencies. These are reradiated to the down-link antenna, providing a closed-loop method of determining approximate zero-set of the range servos prior to each pass. All components in the ground station are inside the calibration loop.

A refinement of the zero-set is made by air link calibration prior to each tracking pass and immediately after each tracking pass. This utilizes a mixer as above and a discone antenna which is 28 meters from the SECOR survey reference mark, and is fed through a cable connected to the ground station.

The difference between the 28-meter surveyed range to the discone and the measured range is recorded on calibration sheets, for both the high-and low-frequency channels, for both precalibration and postcalibration measurements. These calibration numbers are used in the preprocessor to correct the range data.

### 2.3.3 SECOR SYSTEM TIMING

The WICE SECOR station has a rubidium clock. The rubidium clock was used to operate the time code generators which record UTC time on the magnetic tape with a resolution of 1 millisecond each time the digital servos record the range on the tape.

The Wallops Island range time was derived from an HP 5060A cesium clock, set to UTC (NAVOBS). This clock was periodically transported to the SECOR site in order to check the rubidium clock. The offset between the rubidium clock and UTC (NAVOBS), as recorded on the data logs, was always between 5 and 15 microseconds during the WICE operation.

## 2.4 TRANET

The TRANET system was operated by University of Texas personnel under the direction of the Johns Hopkins Applied Physics Laboratory (APL) and the Naval Air Systems Command. The quantity measured by a TRANET tracking system is the doppler frequency as a function of time.

The system concept derives from the fact that, while a spacecraft transmitter sends a continuous unmodulated wave at a fixed frequency, the received signal at the tracking station exhibits a shift in frequency due to the relative velocity of the spacecraft with respect to the observing station. This received frequency is a function of the transmitted frequency, velocity of propagation, and the rate of change of the slant range between the spacecraft and station. The TRANET system located at Wallops has the capability of digitizing the three frequencies from GEOS-2 as well as the two refraction corrected frequencies.

### 2.4.1 TRANET DATA PREPROCESSING

The Naval Weapons Laboratory (NWL) personnel were responsible for the TRANET data preprocessing after collection of the data by APL. The TRANET data undergo the following preprocessing:

- First-order ionospheric refraction corrections are made by analog techniques, using equipment at the tracking station.
- The time of observation is computed. This is defined as the observed time, at the station, of the midpoint of the doppler integration interval. The calibration value (offset of the TRANET station clock from the Wallops Island cesium clock) is used to correct the observation time to UTC (NAVOBS).
- The observation frequency is corrected for the error in the station frequency standard determined from VLF comparisons.
- A spacecraft reference frequency (base frequency) is computed for the pass.
- The data are edited based on a 2.5-sigma rejection criterion.

- The remaining observations are aggregated in groups of eight, covering a 32-second interval. A smoothed frequency value is calculated by fitting a straight line to the residuals in the 32-second interval and evaluating the fit at the central time of the interval. The residual corresponding to the fit at the central time is then added to the computed frequency for that time. These data are run through a reformat program which arranges the filtered data into the format required by the GSDS. All smoothed frequency values and the base frequency for each pass are scaled to 108 megacycles by multiplying by $\frac{108 \times 10^6}{fe}$, where fe is the nominal equivalent frequency obtained from a table. This approximates the frequency out of the station refraction corrector unit.

The TRANET data are the only type of data which undergo mathematical smoothing in these intercomparisons.

The authors received the WICE TRANET data from GSDS and applied the following additional preprocessing steps to the TRANET data prior to intercomparisons with the other systems.

- Converted the recorded time of the observation from observed time at the station to the time the signal was at the satellite by subtracting one-half of the round trip time.

- Converted to range rate values in meters/sec by the following

$$\mathring{R} = \frac{C\,(F_B - F_M)}{F_M}$$

where

$F_B$ = Base frequency received from GSDS

$F_M$ = Smoothed measured frequency received from GSDS

$C$ = Velocity of light

$= 2.997925 \times 10^8$ m/s

- Corrected the range rate values for tropospheric refraction, using the formula

$$\Delta \mathring{R}_T = 0.8432336\, N_s\, \mathring{E} \left[\frac{1 - \sin^2 E}{0.026 + \sin^2 E}\right]^{1/2}$$

$\Delta \overset{\circ}{R}_T$ = correction (cm/sec) to add to R

$N_S$ = ground refractivity, $(1 - \mu)\ 10^6$

E = elevation angle

$\overset{\circ}{E}$ = elevation angle rate (radians/sec)

### 2.4.2 TRANET SYSTEM CALIBRATION

The station frequency error which appears in the doppler data header in the teletype to APL is the departure of the frequency of the station standard as determined from a known (VLF) reference frequency. This known correction is applied, in the NWL preprocessing program, to the frequency measurements. See reference 3.

A nominal value of the satellite oscillator frequency is associated with each spacecraft but is modified for each pass as follows. First, NWL computes O-C's by comparing the VLF corrected doppler frequency measurements with the doppler frequencies predicted from a reference orbit. The reference orbit is determined with previous doppler data from the entire TRANET network. The O-C's are then used to compute an estimated frequency bias for each pass. The spacecraft oscillator nominal frequency corrected for this bias is called the base frequency and is included, as an additional number, with the frequency measurements submitted to the GSDS for each pass.

Since the determination of the base frequency involves the entire TRANET network, the WICE TRANET data are influenced by this network. Data submitted from the other WICE systems are not influenced by any other stations.

### 2.4.3 TRANET SYSTEM TIMING

The station clock error accompanying the doppler data in the teletype to APL combines the station clock offset from the received Wallops Island pulse, the cable delay, and the offset of the Wallops Island working clock (TODG) from the cesium clock. The doppler data submitted to GSDS are referenced to the Wallops Island cesium clock which is set to UTC (NAVOBS).

## 2.5 C-BAND

Data were received from two C-band radars operated by Wallops Island, the AN/FPQ-6 and the AN/FPS-16. Both are pulsed radars capable of nonambiguous

range measurements of up to 32,000 nautical miles, and each provides azimuth and elevation angle measurements to the target. The FPQ-6 radar can also measure range rate ($\dot{R}$) if used with a coherent transponder or if the reflected signal from the spacecraft is strong enough for skin tracking. A passive retro-directive Van Atta array on GEOS-2 makes it possible for the FPQ-6 radar to skin-track this spacecraft.

Two C-band beacons were installed in GEOS-2. Beacon #1 has a 0.7-$\mu$sec fixed nominal delay, and beacon #2 has a 5-usec fixed nominal delay.

The FPQ-6 radar's subsystems may be functionally grouped under signal detection (transmitter, antenna, and receiver), target acquisition, target tracking (range and angle servos), data processing, and system control. An ultrastable frequency-synthesizer-multiplier chain, power amplifier, and hard-tube modulator form the C-band transmitter. The antenna comprises a solid-surface 29-foot parabolic reflector illuminated by a monopulse, polarization-diversified cassegrainian feed. This structure is supported by a 2-axis (azimuth-elevation) pedestal featuring a low-friction hydrostatic azimuth bearing, anti-backlash drive gearing, and precision single-space 20-bit angle-shaft encoding subsystem. The angle, or antenna-positioning, subsystems are high torque-to-inertia electrohydraulic servo loops. Tracking signals are supplied to the antenna-positioning and ranging servos by a low-noise, broad-band, 3-channel receiver subsystem. An all-electronic digital ranging subsystem affords unambiguous range coverage to 32,000 nautical miles at high-pulse-repetition rates, with a granularity of 2 yards. The data system contains a 4096-word coincident-core, bus-organized, stored-program, militarized computer (RCA, FC-4101). (Reference 4.)

The FPS-16 radar is very similar to the FPQ-6 except that it has a 17-bit angle encoder and a 12-foot parabolic reflector and does not have a computer and skin track capability.

### 2.5.1 C-BAND DATA PREPROCESSING

The following preliminary preprocessing is done by Wallops Island:

The on-site RCA 4101 computer program for the AN/FPQ-6 was used to apply the static corrections (pedestal mislevel, droop, nonorthogonality, encoder bias, encoder nonlinearity, and skew) to the raw FPQ-6 data, but not to the FPS-16 data. Dynamic lag corrections calculated by the 4101 program are recorded,

but are not applied to the data. The 4101 FPQ-6 data output tapes and FPS-16 raw data tapes were processed through the Wallops preprocessing program which applies a time tag correction to the data, converts the data from radar bits to range in feet and azimuth and elevation in decimal degrees, and reformats the data from 4101 format to the standard GEOS-B radar data format, sometimes called the modified Calsat format.

WICE C-band data in the modified Calsat format were sent to the Principal Investigator, GEOS OSII. These data were then additionally preprocessed by the WICE C-band preprocessor program at Goddard, which does the following (see Appendix B):

- Computes the time of observation, which is defined as the time when the pulse was at the spacecraft.
- Applies tropospheric refraction corrections to both the range and angle measurements.
- Reformats the data to a format compatible with the GEOS data adjustment program (GDAP). (Editing is done by hand after residuals are obtained with GDAP against the laser reference orbit.)
- Selects every Nth point (one per second).
- Applies range bias corrections derived from the appropriate nominal beacon delay and from the pre- and postpass range target measurements.

### 2.5.2 C-BAND SYSTEM CALIBRATION

For pre- and postmission calibration data tape recorders are run for approximately 10 seconds (at 10 samples/second, this gives approximately 100 samples), recording each of the following:

- Selected AGC values.
- Boresight tower (BST) normal — Antenna electrically locked to the BST in azimuth and elevation.
- Boresite tower plunged — Same set-up as for BST normal, except the antenna is in the plunged mode.

- Range target, skin gate — (If transponder track is planned, the proper delay compensation should be set into range system prior to this step.) Lock on range target in skin gate. Range displays and recordings should read the surveyed range to the range target.
- Range target, beacon gate — Range displays and recordings should read the surveyed range to the range target minus the proper delay compensation.

### 2.5.3 C-BAND SYSTEM TIMING

The received pulse from the Wallops master clock is used by the C-band systems to time-tag the range, azimuth, and elevation data. The circuitry and cable transmission delays bias the time tag by +5.90 milliseconds for the FPQ-6 and +1.05 milliseconds for the FPS-16. These known biases are accounted for in the Wallops program by adding them to the recorded data time tags to give UTC time.

The delay between the Wallops Ce Standard and TODG (200 $\pm$ 100 usec) has not been included thus far in the C-band data time tag corrections. However, these variations are measured and recorded daily at the master site by direct comparison of the TODG oscillator and the cesium beam standard, so the proper correction to the time tag can be applied at some future date.

## 2.6 CAMERAS

Data were taken on GEOS-2 flashes from four BC-4 cameras operated by Wallops Island and one PTH-100 camera operated by Goddard. These data are being processed by Goddard and will be used for future study.

## SECTION 3
## DATA PROCESSING

### 3.1 DATA COMPARISON TECHNIQUES

One method for comparing range (R) and range rate ($\dot{R}$) data from the SECOR, TRANET, and C-band systems with the laser R data is to fit the laser R data with a polynominal in time. This polynominal can be used within the laser data span to produce R and, by differentiation, $\dot{R}$ comparison data at the observation times for the other systems. A small parallax correction must be applied to each data point to account for the difference in location between the laser and the other systems. A similar technique can be employed to compare angle data.

A more convenient method for producing the comparison data at the observation times and for correcting it for parallax is to fit a set of orbital elements ($X_o$, $Y_o$, $Z_o$, $\dot{X}_o$, $\dot{Y}_o$, $\dot{Z}_o$,) to the laser data (or to all the data) and to generate the comparison data from this orbit.

However, in a weighted least-squares fit of an orbit to the data, questions arise as to how to weight the different data sets. For simplicity, and because of gained confidence in the laser data, it was decided to form the reference orbits from laser data alone, zero-weighting all other data. The main disadvantage of this procedure is that the laser data span tends to be short, due to difficulty in tracking GEOS-2 below 20 or 30 degrees elevation angle, and an orbit derived from a short data span is definitive only within the data span.

Also, whereas a short-arc orbit from single-pass R data is good for fitting and reproducing the R data, this orbit will not determine azimuth well. Because of the distance between the FPS-16 and the laser, a 0.5-milliradian (mr) azimuth error in the reference orbit can cause a parallax error of almost a meter in the comparison R data for the FPS-16. Therefore, it is necessary to use angle data, which are good to at least 0.5 mr, along with the laser R data in determining the reference orbits for the FPS-16.

The laser system records azimuth (A) and elevation (E) along with the R data at a one-per-second rate. Based on star tracking and other tests, the laser A, E angles are thought to be accurate to 0.5 mr or better. Therefore, orbits

determined from the laser R,A,E data alone should be adequate for producing smoothed comparison R's for all the other systems, retaining the 1-meter estimated accuracy of the laser R's.

## 3.2 DATUM AND GRAVITY COMPARISON

Previous simulations have shown that, for short-arc orbital fits to data of 1000-second duration or less, using different gravity field coefficients has little effect on the trajectory within the data interval (see reference 8).

Also, it seems intuitively evident that, for systems collocated to within a few kilometers, whose relative positions are known to within $\pm 0.1$ meter, there will be little effect on the trajectory due to expressing the survey in one datum or another prior to generating the laser reference orbits.

However, since several sets of gravity coefficients and several datums are available, some test laser reference orbits were calculated with the GEOS data adjustment program (GDAP), using different gravity coefficients and datums to verify the lack of dependence on these parameters. One set of orbits was run for passes 2,3,5, and 12, using the station locations on the North American datum with zonal gravity coefficients $J_2$ through $J_7$ taken from the NWL-5E6 set. Another set was run for the same passes with the station coordinates converted to the SAO C5 datum, using the techniques described in reference 9 and using the zonals $J_2$ through $J_7$ from the SAO M1 set. The runs are summarized as runs B and C in Table 3-1.

After determining the laser reference orbits both ways, the C-band radar R,A,E observation residuals, with respect to the laser reference orbits, were determined.

Table 3-1
Runs B and C

| Runs | A Priori | OBS. Sigma | Datum | Gravity Set |
|---|---|---|---|---|
| | $\sigma$ R (meters) | $\sigma$ A,E (mr) | | |
| B | 2 | 10 | NAD | NWL-5E6 |
| C | 2 | 10 | SAO-C5 | SAO-M1 |
| D | 2 | 1 | SAO-C5 | SAO-M1 |

Results for pass 5, which exhibited the largest effects on R, are shown in curves B and C in Figure 3-1. Here it can be seen that, for both radars, the change in R residuals between curves B and C within the laser data span is always less than 2 meters and usually less than 1 meter. The change in angle residuals is about 0.20 mr for A data and 0.02 mr or less for E data.

On passes 2, 3 and 12, the effect on R residuals was less than that on pass 5 and the effect on E residuals was about the same as that on pass 5. The A residuals decreased from -11 mr for the B run to -3 mr for the C run for both radars on pass 2, but remained the same on pass 3 (-3.5 mr for both runs) and on pass 12 (+1.6 mr for both runs).

As was expected, the effect on R residuals of the different datums and gravity parameters is small, so either datum or gravity field set can be used for generating the reference orbits. However, in these runs, with the SAO datum and gravity field, the angle residuals for the C-Band radars were either changed by only 0.2 mr or less, as in passes 3,5, and 12, or were significantly decreased, as in pass 2. Furthermore, the SAO set gave better results with camera data in previous long-arc work (see reference 11). Also, the SAO-C5 datum and M1 field were derived together as a consistent set. For these reasons the SAO set was chosen for use in subsequent reference orbit determinations.

## 3.3 LASER DATA WEIGHTING

More test orbits for the same passes were calculated with GDAP to determine how to weight the laser A, E data relative to the laser R data when generating the reference orbits. In the C runs of Table 3-1 and Figure 3-1, the laser R residuals are weighted by multiplication by the reciprocal of the a priori estimate of the R data standard error, $\sigma_R = 2$ meters. Similarly, the laser A, E residuals are weighted by $\sigma_{A,E} = 10$ mr. In the D runs, the relative angle weighting is increased by changing $\sigma_A$ and $\sigma_E$ to 1 mr and keeping $\sigma_R$ at 2 meters. The D curves in Figure 3-1 show little change in the R residuals for the FPQ-6 radar or in the E residuals for either radar, the latter being already well determined to about 0.2 mr. However, the A residuals are reduced from about 5.0 mr to less than 0.5 mr. The independent radar angles are thought to be good to about 0.1 mr. Thus, these radar A, E residuals indicate that the laser reference orbits, weighted as in the D runs,

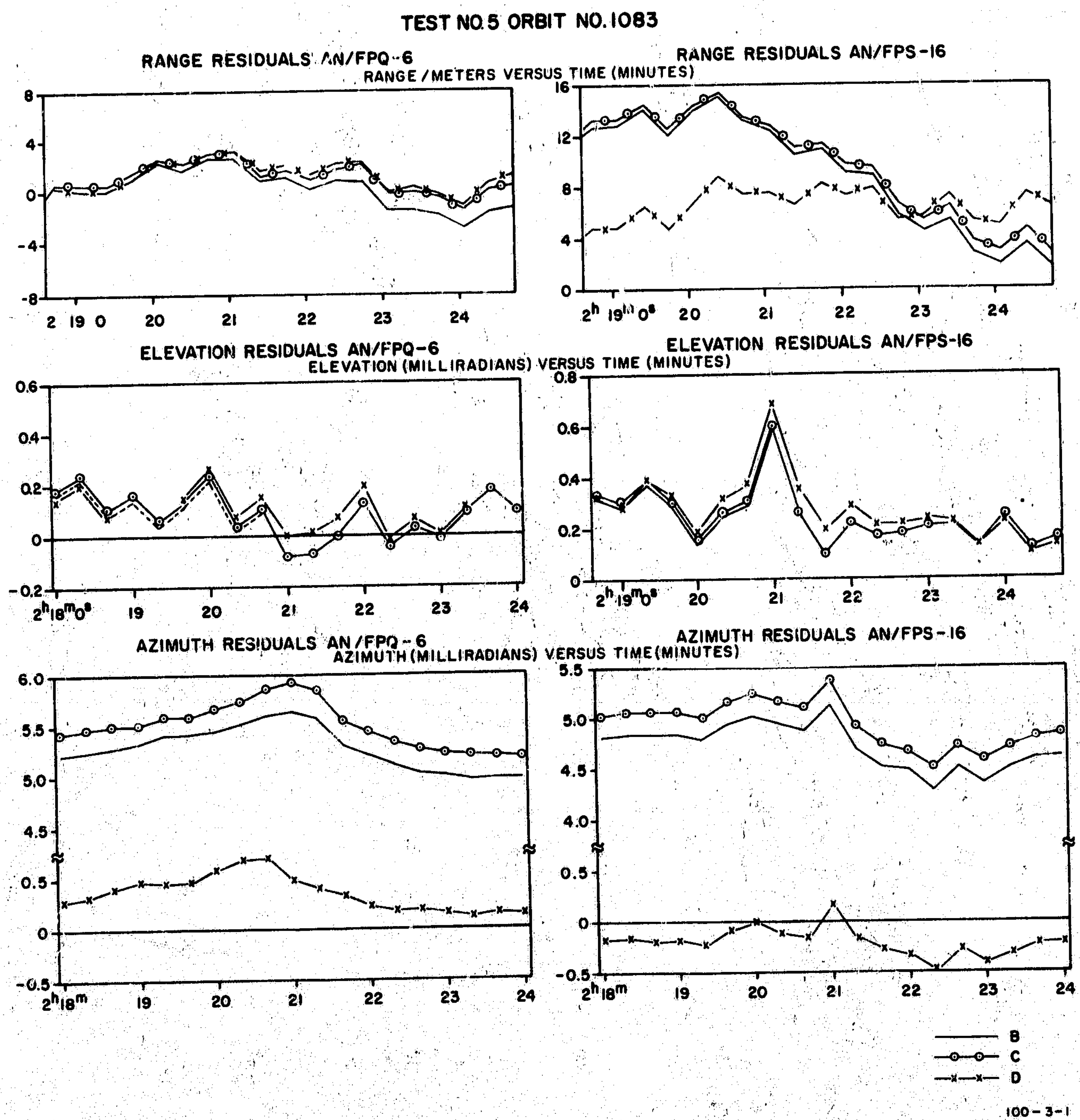


Figure 3-1. Laser Reference Orbits Residuals

produce angles more accurate than the 0.5-mr accuracy attributed to the laser A, E data. Probably the accuracy of the laser angles is more nearly 0.2 to 0.3 mr. This is not accurate enough to evaluate the radar angle data (hopefully, that will be done later when optical camera data become available), but it is accurate enough to suppress parallax errors to below 1 meter when producing comparison R data for the FPS-16 radar. The up-to-7-meter changes in R residuals between the D and C curves for the FPS-16 radar are probably due to parallax errors arising from the 5-mr azimuth bias in the C orbit. Therefore, based on these test cases, the 10 laser reference orbits in this report were all weighted as in the D runs.

## 3.4 LASER REFERENCE ORBITS

In generating the laser reference orbits with GDAP, no atempt is made to recover laser R, A, E observation biases, since previous work indicates this cannot be done reliably (see reference 1). However, the a priori measurement sigmas, $\sigma_R = 2\text{m}$, $\sigma_{A,\,E} = 1$ mr, are chosen conservatively so that, when these propagate via the correlation matrix into the sigmas of the orbital elements, the results will be more realistic.

Having determined a satisfactory method for generating the laser reference orbits, the first 10 laser passes, for which data were available from all systems, were produced, using GDAP. The means and rms fit about the means of the laser R, A, E observations for these 10 orbits are summarized in Table 3-2. The laser R, A, E data residuals are plotted in Figures 3-2, 3-3, and 3-4.

Table 3-2
Laser Reference Orbits

| Date April 1968 | Test # | Orbit # | Laser Interval (sec) | Range (Meters) A Priori rms | Range A Posteriori mean | Range A Posteriori rms | Azimuth (milliradians) rms | Azimuth A Posteriori mean | Azimuth A Posteriori rms | Elevation (milliradians) rms | Elevation A Posteriori mean | Elevation A Posteriori rms |
|---|---|---|---|---|---|---|---|---|---|---|---|---|
| 2 | 2 | 1044 | 231 | 2 | .000 | 1.3 | 1 | .000 | 0.22 | 1 | -0.045 | 0.11 |
| 3 | 3 | 1057 | 265 | 2 | .001 | 1.0 | 1 | .000 | 0.48 | 1 | -0.072 | 0.14 |
| 5 | 5 | 1083 | 367 | 2 | .001 | 1.0 | 1 | .002 | 0.40 | 1 | -0.183 | 0.21 |
| 10 | 9 | 1147 | 113 | 2 | .000 | 1.4 | 1 | .000 | 1.17 | 1 | -0.027 | 0.19 |
| 12 | 11 | 1173 | 386 | 2 | .000 | 1.2 | 1 | .001 | 0.31 | 1 | -0.049 | 0.21 |
| 13 | 12 | 1186 | 266 | 2 | .000 | 1.1 | 1 | .000 | 0.21 | 1 | +0.030 | 0.15 |
| 16 | 14 | 1224 | 315 | 2 | .002 | 1.2 | 1 | -.001 | 0.74 | 1 | -0.171 | 0.15 |
| 17 | 15 | 1237 | 445 | 2 | .000 | 1.3 | 1 | .000 | 0.63 | 1 | +0.143 | 0.20 |
| 18 | 16 | 1250 | 59 | 2 | .000 | 1.7 | 1 | .000 | 0.24 | 1 | -0.007 | 0.08 |
| 20 | 18 | 1275 | 165 | 2 | .000 | 1.4 | 1 | .000 | 0.14 | 1 | -0.002 | 0.12 |
| Average | | | 261 | | .000 | 1.3 | | .000 | 0.45 | | -0.038 | 0.16 |

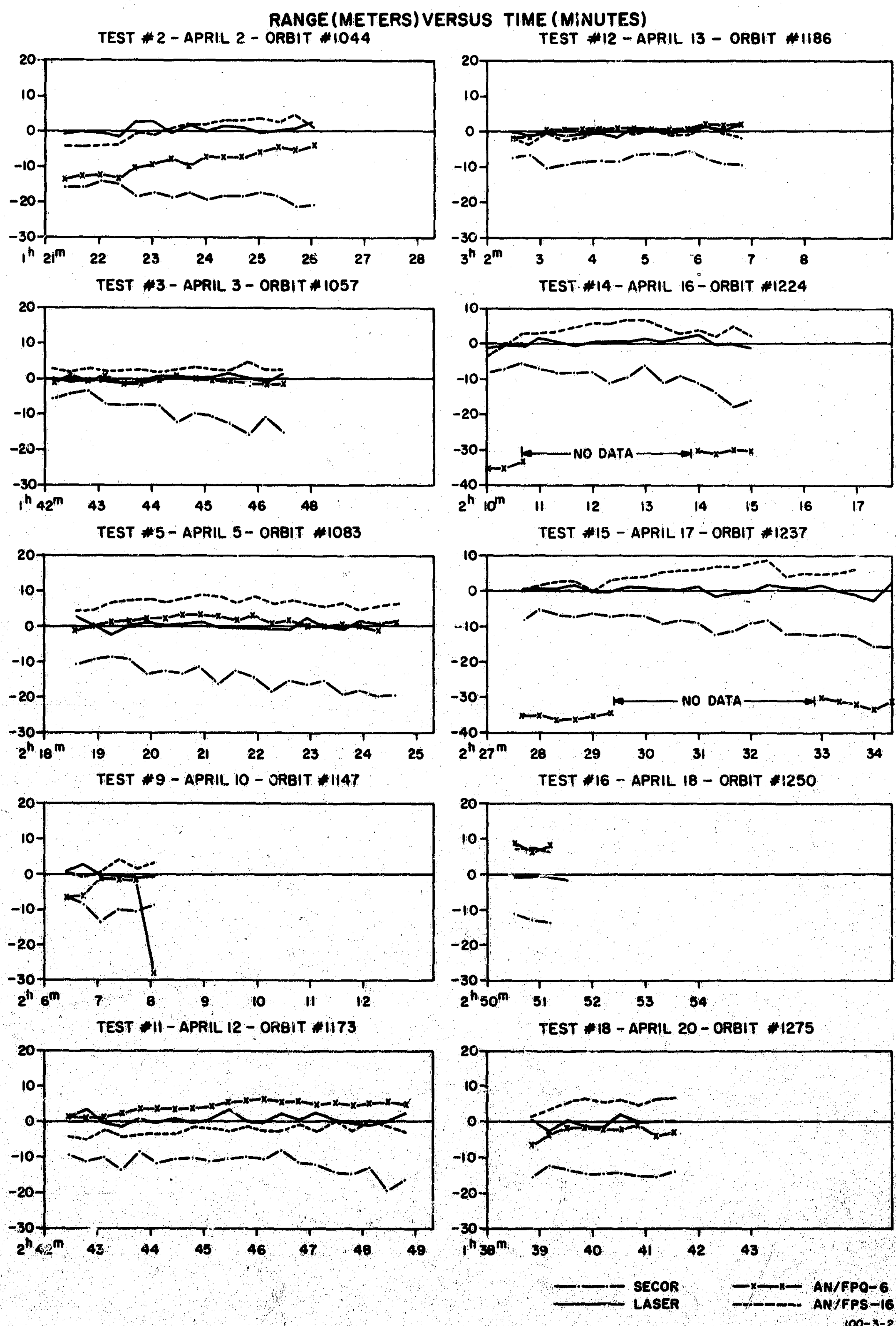


Figure 3-2. Range Residuals

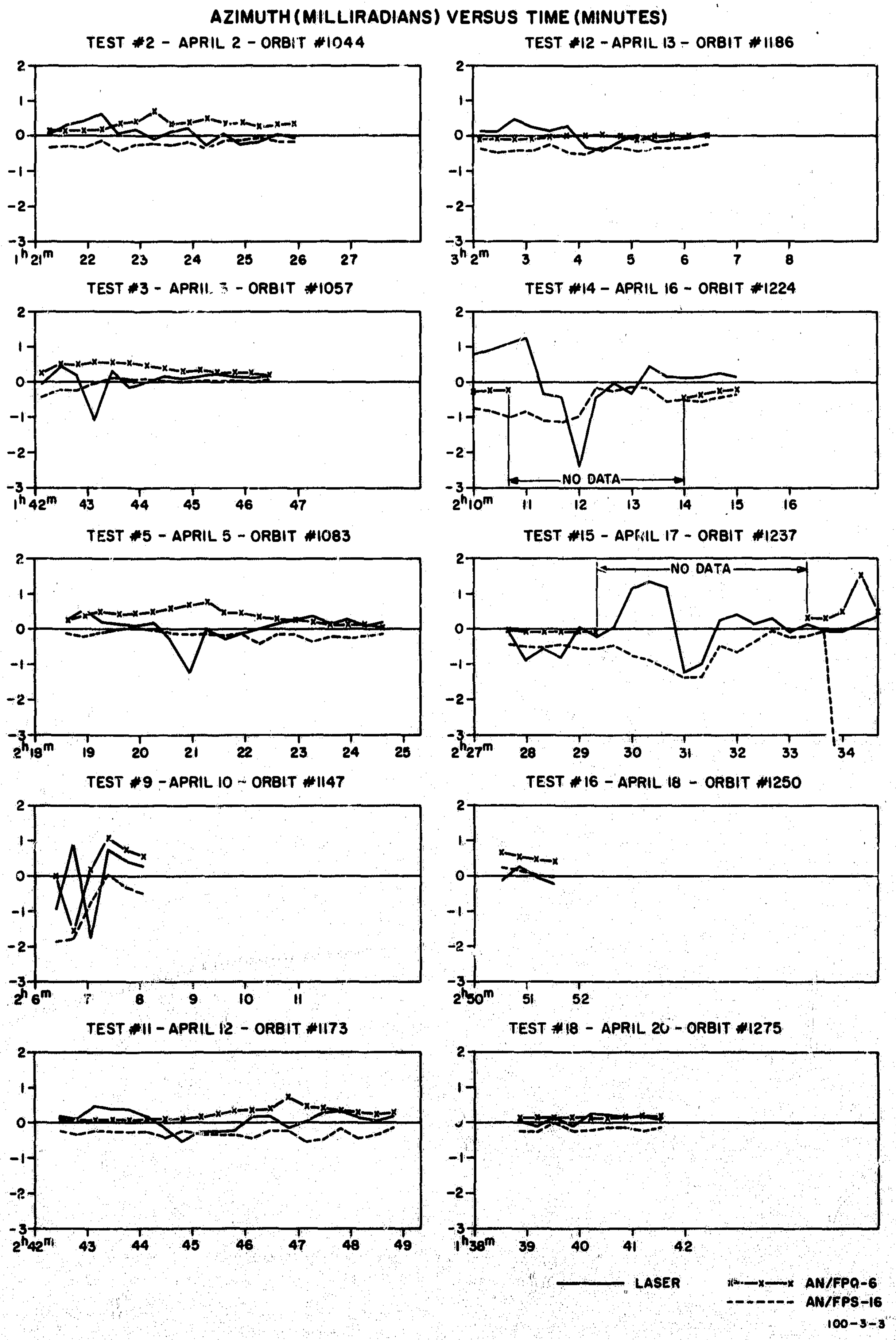


Figure 3-3. Azimuth Residuals

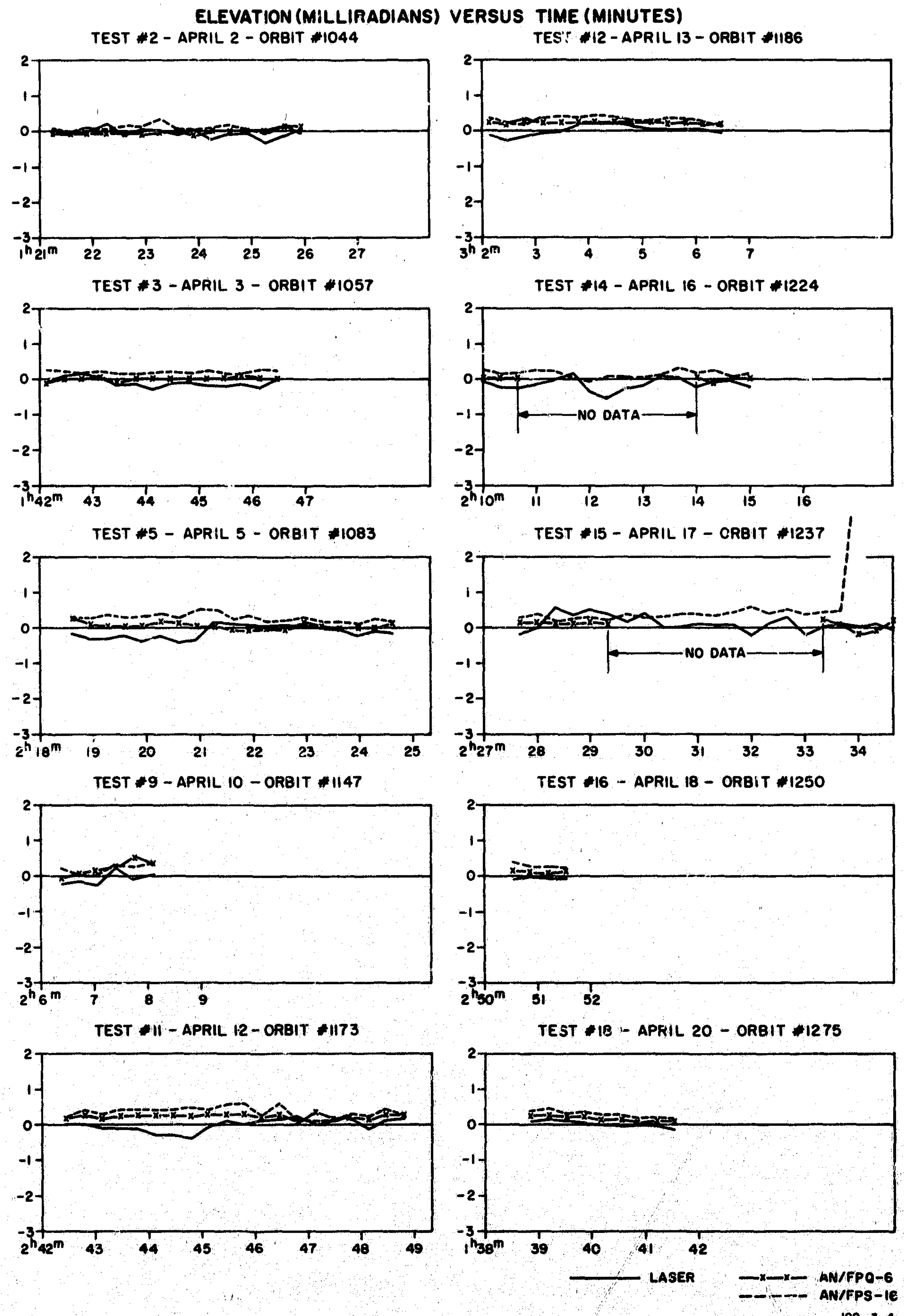


Figure 3-4. Elevation Residuals

## 3.5 SYSTEM ERROR MODELS

After determining the laser reference orbits, GDAP is used again to form observation residuals (O–C) between the preprocessed observations (O) from each measurement channel and the calculated values (C) from the reference orbits. GDAP is then used to minimize the weighted observation and parameter residuals for each channel in a least-squares adjustment of the error model coefficients, with the previously derived laser reference orbital elements held fixed. The observation and parameter residuals are weighted according to the a priori estimates of the sigmas of the observations and parameters.

The error models used in this study are very simple. They consist of a zero-set and a timing bias for each R and $\overset{\circ}{R}$ channel, and only a zero-set bias for each A and E channel. Thus, the linear error model assumed for each measurement channel is the following:

$$(O-C)_i = B + T \cdot \overset{\circ}{O}_i + \xi$$

where $(O-C)_i$ = known observation channel residual for each data point, determined as explained above

$B$ = unknown zero-set bias coefficient, assumed constant for a pass

$\overset{\circ}{O}_i$ = known time rate of change of observation data, determined from the reference orbit

$T$ = unknown time bias coefficient, assumed constant for a pass. In this study T=0 was assumed for the angle channels

$\xi$ = random error in the measurement

For each measurement channel, a value of $\overset{\circ}{O}$ and a value of (O–C) are calculated for each of the n observations. Conceptually, the problem then is to solve, by least squares, for the slope, T, and intercept, B, of the straight line fit to the plot of the n values of (O–C) versus $\overset{\circ}{O}$ or, in other words, to solve the n linear equations, by least squares, for the two unknown coefficients, B and T.

The *a priori* estimates of the measurement sigmas are given in Table 3-3.

Table 3-3
A Priori Estimates

| System | R | A | E | $\dot{R}$ |
|---|---|---|---|---|
| SECOR | 30m | | | |
| FPQ6 | 30m | 0.1mr | 0.1mr | |
| FPS16 | 30m | 0.1mr | 0.1mr | |
| TRANET | | | | 4 cm/sec |

The *a priori* values for the zero-set and timing bias sigmas were all set very large in order to leave these parameters unconstrained.

## 3.6 INTERCOMPARISON RESULTS

The results of the system intercomparisons are summarized in Tables 3-2 and 3-4 through 3-6 and Figures 3-2 through 3-5. The tables give the mean and rms about the mean for the observation residuals after allowing for a zero-set bias and, in the case of the R and $\dot{R}$ data, after allowing for a time bias also. The values of the zero-set and time biases are given for each measurement channel on each pass. Then an average bias for each channel is calculated for all 10 passes. The figures show the measurement residuals with respect to the laser reference orbits prior to adjusting for the zero-set and timing biases.

### 3.6.1 LASER

For the 10 laser passes, the average pass length from Table 3-2 is 261 seconds. The averages, over the 10 passes, of the mean and rms about the mean for the laser R, A, E data are as follows:

| | R (meter) | A (mr) | E (mr) |
|---|---|---|---|
| Mean | 0.000 | 0.000 | -0.038 |
| RMS | 1.3 | 0.45 | 0.16 |

3.6.2 SECOR

The average SECOR range rms, zero-set bias, timing bias, and standard deviations for the biases for the 10 passes, as given in Table 3-4, are:

rms 1.7 meters

B $-10.8 \pm 3.4$ meters

T $-0.78 \pm 0.74$ milliseconds

These values are derived from the SECOR data on the third SECOR tape submitted to the GSDS. SECOR data were submitted to GSDS three times as the Army Map Service (AMS) made changes to its preprocessing procedures.

The first SECOR data tape submitted to the GSDS contained SECOR data coincident with the first 5 laser passes. The data on this tape were given the usual preprocessing treatment by AMS, as described earlier. Results from GDAP were compared with AMS results which were obtained from the AMS independent computer program. These were found to be consistent to within 1 meter, although the SECOR range readings were about 10 meters shorter than the laser ranges.

In trying to find the cause of the 10-meter bias between the laser and SECOR data, AMS reviewed its preprocessing procedures and decided to resubmit the data with 3 slight changes. The second SECOR data tape contained 6 passes and the following 3 changes to the preprocessing:

- A scale factor change of about $1 \times 10^{-6}$ was made to the R data to account for the time-counting frequency in the SECOR being scaled to a different value of the velocity of light than is used by the laser. The laser uses c = 299792.5 km/sec.
- A 1/2-millisecond bias was added to the recorded time tag. The SECOR data time tag displays the current time truncated at 1 millisecond. The SECOR procedure at Wallops Island was to keep this data time tag at a constant millisecond reading throughout the pass by adjusting the transmission time of the read-out signal. To stay within the limits of a 1-millisecond truncated time display, the operator will presumably try to remain centered in the allowable display interval of 1 millisecond. Hence, on the average, the data read-out occurs 1/2 millisecond after the displayed and recorded time tag. This time correction is required only when SECOR data are to be correlated with data from other systems as in these tests.

Table 3-4
Range Data Comparisons

| TEST # | Range (Meters) | | | | | | | | | Time Bias (milliseconds) | | |
|---|---|---|---|---|---|---|---|---|---|---|---|---|
| | SECOR | | | AN/FPQ-6 | | | AN/FPS-16 | | | | | |
| | mean | rms | zero-set bias | mean | rms | zero-set bias | mean | rms | zero-set bias | SECOR | AN/FPQ-6 | AN/FPS-16 |
| 2 | .000 | 1.6 | -18.6 | .000 | 1.4 | -8.9 | .000 | 2.1 | -0.1 | -0.58 | 0.80 | 0.67 |
| 3 | .000 | 2.4 | -6.1 | .000 | 0.7 | -0.3 | .000 | 1.0 | 2.6 | -1.38 | -0.02 | -0.04 |
| 5 | .000 | 1.7 | -13.5 | .000 | 1.2 | 1.4 | .021 | 1.5 | 6.6 | -0.94 | -0.11 | -0.01 |
| 9 | .000 | 1.8 | -9.4 | - | - | - * | .000 | 1.0 | 1.2 | -0.35 | - | 0.78 |
| 11 | .000 | 2.2 | -11.5 | .000 | 1.1 | 5.2 | .000 | 1.2 | -1.9 | -0.29 | 0.41 | 0.26 |
| 12 | .000 | 1.6 | -8.1 | .000 | 0.6 | 0.7 | .000 | 1.1 | -1.0 | 0.10 | 0.52 | 0.31 |
| 14 | .000 | 1.9 | -9.5 | .000 | 0.9 | -33.1* | .000 | 2.1 | 2.9 | -0.59 | 0.50 | 0.57 |
| 15 | .000 | 1.9 | -10.4 | .000 | 1.1 | -33.7* | .000 | 1.7 | 4.7 | -0.73 | 0.33 | 0.44 |
| 16 | .000 | 0.9 | -8.0 | .000 | 0.7 | 7.8 | .000 | 0.8 | 7.5 | -2.67 | 0.34 | 0.16 |
| 18 | .000 | 1.2 | -13.3 | .000 | 1.1 | -3.6 | .000 | 1.0 | 4.3 | -0.32 | 0.56 | 0.49 |
| Average | | 1.7 | -10.8 ±3.4 | | 1.0 | 0.3 ±5.1** | | 1.4 | 2.7 ±3.0 | -0.78 ±0.74 | 0.37 ±0.27 | 0.33 ±0.25 |

*Skin-track Passes
**Skin-track Passes Were Not Included in This Average

Table 3-5
Angle Data Comparisons Angle (Milliradians)

| Test # | AN/FPQ-6 | | | | | | AN/FPS-16 | | | | | |
|---|---|---|---|---|---|---|---|---|---|---|---|---|
| | Azimuth | | | Elevation | | | Azimuth | | | Elevation | | |
| | mean | rms | zero-set bias | mean | rms | zero-set bias | mean | rms | zero-set bias | mean | rms | zero-set bias |
| 2 | .000 | 0.12 | 0.30 | .000 | 0.06 | 0.03 | .000 | 0.12 | -0.22 | .000 | 0.11 | 0.09 |
| 3 | .000 | 0.13 | 0.39 | .000 | 0.04 | 0.06 | .000 | 0.18 | -0.06 | .000 | 0.08 | 0.16 |
| 5 | .000 | 0.18 | 0.36 | .000 | 0.09 | 0.10 | .000 | 0.14 | -0 20 | .000 | 0.12 | 0.26 |
| 9 | — | — | — | — | — | — | .000 | 0.76 | -0.70 | .000 | 0.14 | 0.17 |
| 11 | .000 | 0.17 | 0.23 | .000 | 0.06 | 0.24 | .000 | 0.13 | -0.30 | .000 | 0.14 | 0.34 |
| 12 | .000 | 0.05 | -0.05 | .000 | 0.03 | 0.28 | .000 | 0.06 | -0.41 | .000 | 0.05 | 0.34 |
| 14 | .000 | 0.29 | 0.13 | .000 | 0.04 | 0.06 | .000 | 0.40 | -0.62 | .000 | 0.14 | 0.11 |
| 15 | .000 | 0.34 | 0.21 | .000 | 0.10 | 0.13 | .000 | 0.40 | -0.58 | .000 | 0.28 | 0.35 |
| 16 | .000 | 0.07 | 0.53 | .000 | 0.05 | 0.12 | .000 | 0.09 | 0.03 | .000 | 0.06 | 0.02 |
| 18 | .000 | 0.04 | 0.18 | .000 | 0.07 | 0.16 | .000 | 0.08 | -0.22 | .000 | 0.12 | 0.27 |
| Average | | 0.15 | 0.25 ± 0.16 | | 0.06 | 0.13 ± 0.08 | | 0.24 | -0.34 ± 0.25 | | 0.12 | 0.21 ± 0.11 |

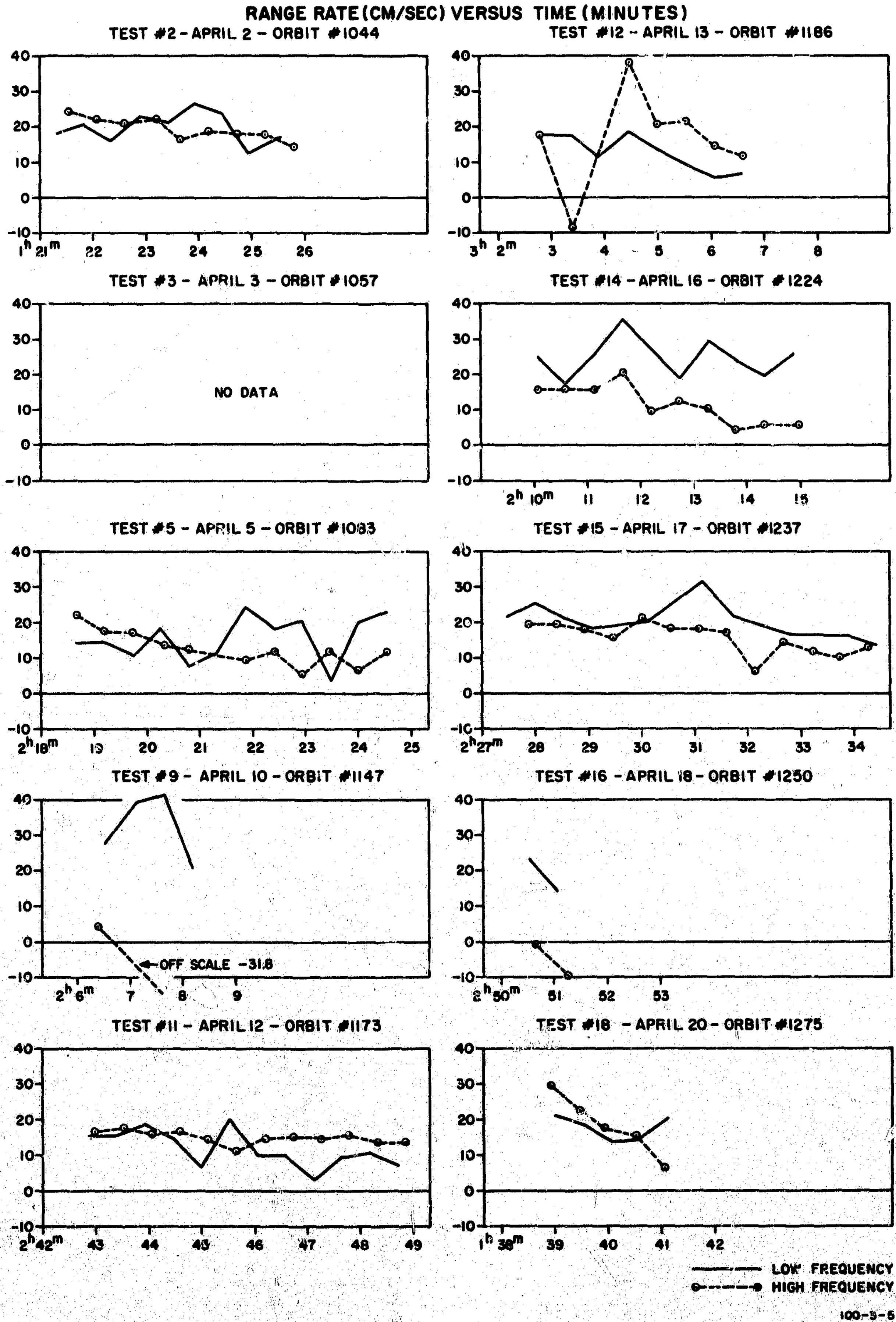


Figure 3-5. Range Rate Residuals

RANGE/METERS VERSUS TIME (MINUTES)

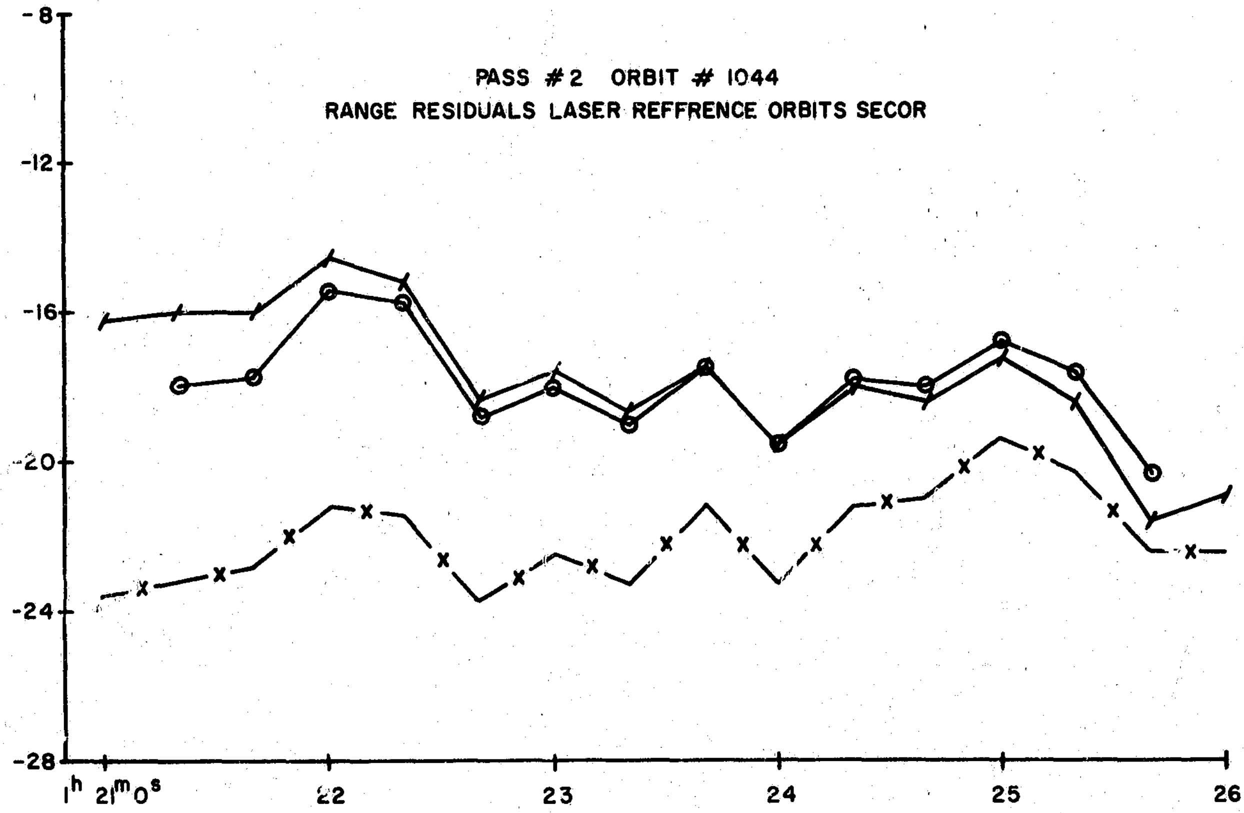



Figure 3-6. SECOR Range Residuals

- Pre- and postcalibration ranges were taken from the magnetic data tape rather than the handwritten logs to reduce the possibility of human error.

The third SECOR data tape had 10 passes and one additional preprocessing step.

- The tropospheric refraction correction was applied to the ambiguity-corrected ranges rather than to the raw ranges as had been done previously.

In Figure 3-6, SECOR R residuals with respect to the laser reference orbit for passes 2 and 3 are plotted from each of the three SECOR tapes to give an idea of the effect of the preprocessing changes.

These preprocessing changes are discussed here only because they illustrate how careful one must be with both the system operating procedures and the data preprocessing when comparing systems as potentially accurate as the geodetic SECOR. Also, the stimulation of a procedural review and the subsequent discovery of better preprocessing methods is a valuable result of a systems intercomparison study such as this.

### 3.6.3 C-BAND

The averages from Table 3-4, -5 for the C-band radars from 10 WICE passes are:

| Averages | AN/FPQ-6 | | AN/FPS-16 | |
|---|---|---|---|---|
| | rms | bias | rms | bias |
| Range (meters) | 1.0 | 0.3 ± 5.1 | 1.4 | 2.7 ± 3.0 |
| Azimuth (mr) | 0.15 | 0.25 ± 0.16 | 0.24 | -0.34 ± 0.25 |
| Elevation (mr) | 0.06 | 0.13 ± 0.08 | 0.12 | 0.21 ± 0.11 |
| R time bias (ms) | -- | 0.37 ± 0.27 | -- | 0.33 ± 0.25 |

The range averages for the AN/FPQ-6 did not include passes 9, 14, and 15, which were skin-tracks. Pass 9 is a short pass and only skin-track data were obtained during the laser interval. The AN/FPQ-6 radar is a centroid tracker, and any difference in the pulsewidth used for calibration and the pulsewidth experienced in tracking will result in a range bias error (reference 6). For GEOS-2 combined

beacon/skin missions, the AN/FPQ-6 was calibrated, using a 1-usec pulsewidth, and the beacon portion of the mission was tracked, using the same 1-usec pulsewidth, while the actual transponder reply was 0.6 usec. The 0.2-usec difference between the two centroids results in a range bias of 29.98 meters which must be added to the data. This range bias has been computed from the approximate value of the pulsewidths, and in that respect, the bias of 33 meters obtained for passes 14 and 15 is consistent with this explanation.

On skin-track, the FPQ-6 radar measures both R and $\mathring{R}$ which, it is hoped, will be examined later. In this report, only the beacon track R data are evaluated.

To help verify the GDAP results, Laser reference orbits and C-band residuals were also computed in the NONAME program for all 10 passes. Identical inputs and procedures were used. The NONAME program was developed for Goddard long-arc orbital studies and differs from GDAP in many ways. Some of the major differences are:

- NONAME employs the full SAO MI gravity field model plus selected resonant terms for GEOS
- NONAME includes corrections for solar radiation pressure, drag, lunar, and solar perturbations
- NONAME employs a different reference coordinate system than GDAP
- NONAME operates on the IBM-360 computer, whereas GDAP operates on the CDC-3200

Over all 10 passes for both radars, the largest single-point discrepancy in C-band R data residuals between the GDAP and NONAME runs was about 1.3 meters. The average discrepancy was, more nearly, only 0.1 meter.

Furthermore, mean differences between the radars and between the radar and the laser R data, reported by Wallops Island in reference 6 for passes 5, 12, and 18, differed from GDAP-derived R bias determinations by, at most, 1.6 meters, with an average difference over the 3 passes of only 0.1 meter for the FPS-16 and 0.5 meter for the FPQ-6. Wallops used the same NONAME computer program, but derived reference orbits from the FPQ-6 data rather than from the laser data, as was done with GDAP.

### 3.6.4 TRANET

The TRANET data are submitted to the GSDS for both a low-frequency (162:324 MHz) and a high-frequency (324:972 MHz) pair. In effect, the two frequency pairs may be considered to be from two collocated, but distinct, stations, although some equipment, such as the station clock, is common to both frequency pairs. In this study the two frequency pairs were treated as two distinct stations.

The TRANET B and T bias recovery runs were made with the NONAME program, using laser reference orbits from previous NONAME runs. Later, these will be rerun on GDAP for additional verification. The laser reference orbits were generated in NONAME, using the same procedures as in GDAP. That is, the same a priori laser R, A, E measurement sigmas were used, and no attempt was made to recover laser biases.

In the NONAME bias recovery runs, the 6 orbital elements must be considered as unknowns, along with the B and T biases for the two TRANET stations, although the orbital elements may be tightly constrained. Thus, the 6 orbital elements and 4 biases require at least 10 TRANET data points, or 5 points from each station, in order to obtain a solution. Passes 9 and 16 were too short to obtain a solution, since the smoothed TRANET data points are available only once per 32 seconds. For pass 3, no TRANET data were available.

For the remaining passes, the first bias recovery runs used tightly constrained orbital elements ($\pm 10^{-2}$ meters in position, $\pm 10^{-6}$ meters/sec in velocity) and assumed the following a priori estimates of measurement and bias sigmas for both TRANET stations:

| | |
|---|---|
| rms | 4 cm/sec |
| B | 1000 cm/sec |
| T | 50 ms |

As might have been anticipated, the correlation between B and T was high (93%) over the short laser data spans, and the sigma of the B and T recovery was larger than desired ($\pm$3.4 cm/sec for B, $\pm$ 1.2 ms for T). This means that, when the $\mathring{R}$ residuals curve is plotted against time, the bell-shaped curve, characteristic of a T bias, cannot be distinguished from a horizontal line, characteristic of a B bias, at least over the central part of the curve covered by the laser data span.

To obtain better estimates of B or T, it is necessary to either extend the residuals curve far enough to bring out the difference between the B and T characteristic curves or to constrain either B or T and solve for the other. In this study, advantage was taken of the well-controlled synchronization between the laser and TRANET clocks to constrain the TRANET T for both TRANET stations to 0.1 ms rather than the 50.0 ms used before.

The passes were rerun with the 0.1-ms T constraint, and the results are given in Table 3-6. Now the estimated error in the B recovery lies between 1.1 and 1.8 cm/sec. The average results from Table 3-6 are given below. The uncertainty in the average B and T values quoted below is the standard deviation of the set of derived B and T values, not the average of the estimated errors. The $\dot{R}$ rms values were not calculated in NONAME unless at least 10 $\dot{R}$ data points were available.

| | Low Frequency | High Frequency |
|---|---|---|
| RMS | 5.39 cm/sec | 4.09 cm/sec |
| B | 17.59 ± 4.53 cm/sec | 15.60 ± 2.78 cm/sec |
| T | 7 ± 9 usec | 5 ± 7 usec |

In discussions with Naval Weapons Laboratory (NWL) personnel concerning the large values of B bias derived from these runs, it was revealed that most of the bias could be accounted for by a procedure in the preprocessing program at NWL. In this program, the propagation time correction between station and spacecraft is not applied to the data. This results in biasing the value of base frequency ($f_B$) submitted with the data to the GSDS. This procedure is peculiar only to the GEOS (and ANNA) preprocessing program and, therefore, affects the TRANET data in the GSDS, but not the TRANET data as normally used at NWL.

Corrections to the base frequency ($\Delta f_B$) were provided, by NWL, for the low-frequency pair on most of the 10 WICE passes. NWL obtained the $\Delta f_B$'s by recalculating the TRANET residuals with respect to TRANET reference orbits after correcting for the propagation time delay but without correcting for tropospheric refraction. The new residuals were then used to derive new base frequencies. The NWL base frequency corrections, $\Delta f_B$, are given in Table 3-7. These corrections are converted to range rate corrections, using the conversion factor in Table 3-7.

The converted NWL corrections are then compared with the TRANET $\mathring{R}$ bias values which were derived in this report by comparison with the laser reference orbits. The NWL corrections agree, in general, with the laser-derived corrections, but on the average, they are larger by 4.8 cm/sec for the low-frequency TRANET pair. Since this type of bias apparently affects all the TRANET data in the GSDS, it is necessary to allow for a bias when doing geodetic calculations with the data. Even with the NWL corrections to the base frequency, it is still advisible to allow for a bias when using TRANET data.

Table 3-6
Range Rate Data Comparisons

| Pass Number | rms (low) (cm/sec) | bias (low) (cm/sec) | time (low) (milliseconds) | rms (high) (cm/sec) | bias (high) (cm/sec) | time (high) (milliseconds) |
|---|---|---|---|---|---|---|
| 2 | | 19.67 | 0.007 | | 19.41 | -0.003 |
| 3 | | No doppler | | | | |
| 5 | 6.27 | 15.84 | -0.007 | 4.90 | 12.68 | -0.003 |
| 9 | | Too short | | | | |
| 11 | 4.76 | 11.23 | 0.008 | 1.84 | 14.82 | 0.000 |
| 12 | | 12.51 | 0.005 | | 16.54 | 0.008 |
| 14 | | 24.46 | 0.008 | 5.35 | 11.35 | 0.019 |
| 15 | 5.13 | 20.93 | 0.027 | 4.28 | 15.45 | 0.004 |
| 16 | | Too short | | | | |
| 18 | | 18.46 | 0.000 | | 19.01 | 0.009 |
| | 5.39 | 17.59 ± 4.35 | 0.007 ± .009 | 4.09 | 15.60 ± 2.78 | 0.005 ± .007 |

<u>A Priori</u>

| Measurement | Bias | Time |
|---|---|---|
| 4 cm/sec | 10 m/sec | 0.1 millisecond |

<u>A Priori</u> Variance on the Orbital Elements

| | | |
|---|---|---|
| VX | 0.0001 | meters$^2$ |
| VY | 0.0001 | meters$^2$ |
| VZ | 0.0001 | meters$^2$ |
| $V\mathring{X}$ | $10^{-12}$ | meters$^2$/sec$^2$ |
| $V\mathring{Y}$ | $10^{-12}$ | meters$^2$/sec$^2$ |
| $V\mathring{Z}$ | $10^{-12}$ | meters$^2$/sec$^2$ |

Table 3-7
Comparison of NWL Bias Corrections with Laser-derived Biases (B)

| Pass | $\frac{\text{Lo } \Delta f_B}{(10^{-3} \text{ Hz})}$ | $\Delta \mathring{R} = -C \frac{\Delta f_B}{f_B}$* Lo (cm/sec) | Lo B (cm/sec) | $\Delta \mathring{R}$-B Lo (cm/sec) |
|---|---|---|---|---|
| 2 | — | — | 19.67 | — |
| 5 | -61 | 16.94 | 15.84 | 1.10 |
| 9 | -78 | — | — | — |
| 11 | -95 | 26.39 | 11.23 | 15.16 |
| 12 | -62 | 17.22 | 12.51 | 4.71 |
| 14 | -77 | 21.39 | 24.46 | -3.07 |
| 15 | -86 | 23.89 | 20.93 | 2.96 |
| 16 | -90 | — | — | — |
| 18 | -95 | 26.39 | 18.46 | 7.93 |
| | | Average | | 4.80 |

*C = 300 x $10^8$ m/sec
$f_B$ (Lo) = 108 MHz

# SECTION 4
# ERROR PROPAGATION STUDY

The GDAP and NONAME programs calculate, along with the estimate of each bias value, an estimate of the error or sigma in that value. The resulting error estimate is based on the a priori estimates of both the measurement sigmas and the bias sigmas. These error estimates are not given in Tables 3-4 and 3-5 because the a priori measurement sigmas used (see Table 3-1) were not realistic, particularly the estimate of 30 meters for the sigma of the range channels. Also, since the laser reference orbits were held fixed, the estimated error in the laser angles is not propagated into the bias sigma estimates as it should be.

To determine more accurate estimates of the error in the recovered B and T values, special error propagation runs were made with NONAME, using more realistic a priori measurement sigmas and bias sigmas. Also, the orbital elements, although still dominated by the laser data, were allowed to adjust, thereby propagating the effect of the laser measurement sigmas and laser bias sigmas into the B and T error estimates for the other channels. Approximate average measurement sigmas were taken from the results given in Tables 3-2 and 3-4 through 3-6 for all 10 passes and used as a priori estimates of the measurement sigmas in these special runs. The a priori measurement sigmas and bias sigmas selected for these runs are summarized in Table 4-1. For all but the laser and camera data, the a priori bias sigmas were chosen large so as not to constrain the final estimate of these sigmas. For these runs, the laser R, A, E data channel biases are also admitted into the solution. These are assigned a priori bias sigma estimates of 1 meter in range and 100 seconds of arc in angle. These are thought to be realistic or even pessimistic estimates. However, these a priori values will dominate all the resulting estimates of the bias sigmas.

No adjustment is allowed for the laser clock, since one system clock must be the reference to which the other T estimates are referred.

A difference between the NONAME and GDAP T solutions is that, in the NONAME solutions, for the C-band radars, all measurement channels (R, A, E) common to each radar contribute to recovery of the T bias for the radar, whereas in the GDAP solutions, a T bias recovery was attempted only for the R channel.

For reasons similar to those discussed in paragraph 3.6.4, the runs were first done with an *a priori* T sigma estimate of 50 ms for TRANET, and then repeated with the 50 ms replaced by a 0.1-ms estimate.

These runs were made with data from passes 3 and 5, and only data within the laser data span were used. Pass 3 was used because optical data from a single plate from the collocated PTH-100 camera were available for that pass. Unfortunately, TRANET data, although taken for that pass, were not submitted to the GSDS. Pass 5 was used because data from all the WICE radio systems were available for that pass. However, no optical data were available for pass 5.

The results of the error propagation runs are given in Table 4-2 for the calculated measurement sigmas and in Table 4-3 for the calculated B and T bias estimates and sigmas of those estimates.

As was anticipated, the laser *a priori* estimate of one meter for R bias sigma dominates the error estimates for R bias recovery for the other systems. Similarly, the laser *a priori* estimate of 0.5 mr or 103 arc-sec for azimuth (A) bias sigma dominates the error estimates for the A bias recovery. However, when the data from the single camera plate are introduced, the A bias error estimates are reduced to from 3 to 6 arc-sec. Interestingly, the sigmas of E angle biases for the laser and C-band radars are already down to 1 to 2 arc-sec even before the optical data are introduced.

The sigmas of the T estimates for SECOR and the C-band radars were calculated to be about 0.1 ms with or without the camera data. For TRANET, with an *a priori* sigma of the T estimate of 50 ms, the calculated sigma of the T estimate is about 1.2 ms, and the calculated sigma of the $\mathring{R}$ bias is about 3.4 cm/sec for pass 5. Reducing the *a priori* sigma of the T estimate for TRANET to 0.1 ms reduces the calculated sigma of the $\mathring{R}$ bias to about 1.2 cm/sec. It can be shown that equally small values of the sigma of the $\mathring{R}$ bais can be obtained without the need for constraining the *a priori* sigma of the T estimate by extending the data span.

Table 4-1
A Priori Inputs to Error Propagation Runs

| Measurement Sigmas | | | | |
|---|---|---|---|---|
| System | R(m) | A($\widehat{sec}$) | E($\widehat{sec}$) | $\mathring{R}$(cm/sec) |
| Laser | 2 | 90 | 30 | |
| FPQ-6 | 2 | 30 | 12 | |
| FPS-16 | 2 | 50 | 25 | |
| SECOR | 2 | — | — | |
| TRANET | — | — | — | 4 |
| Camera ($\alpha$, $\delta$) | | 2 | 2 | |

| Bias Sigmas | | | | | |
|---|---|---|---|---|---|
| System | R(m) | A($\widehat{sec}$) | E($\widehat{sec}$) | $\mathring{R}$(cm/sec) | T(ms) |
| Laser | 1 | 100 | 100 | | — |
| FPQ-6 | 100 | 1000 | 1000 | | 50 |
| FPS-16 | 100 | 1000 | 1000 | | 50 |
| SECOR | 100 | | | | 50 |
| TRANET (Lo & Hi) | | | | 1000 | 50.0 |
| TRANET (Lo & Hi) | | | | 1000 | 0.1 |
| Camera (A, E$\rightarrow\alpha,\delta$) | | — | — | | |

Table 4-2
Measurement Sigmas Resulting from Error Propagation Study

| System | Pass | R(m) | A($\widehat{sec}$) | E($\widehat{sec}$) | $\dot{R}$(cm/sec) | Time Bias (ms) |
|---|---|---|---|---|---|---|
| Laser | | 2. | 90 | 30 | | |
| | 5 | 1.13 | 75.4 | 43.7 | | |
| | 3 | 1.01 | 65.3 | 27.7 | | |
| | 3* | 1.01 | 64.5 | 28.0 | | |
| FPQ-6 | | 2. | 30. | 12. | | |
| | 5 | 0.73 | 26.3 | 16.9 | | |
| | 3 | 0.71 | 24.1 | 8.1 | | |
| | 3* | 0.70 | 28.8 | 8.2 | | |
| FPS-16 | | 2. | 50. | 25. | | |
| | 5 | 0.98 | 21.5 | 21.6 | | |
| | 3 | 0.97 | 36.1 | 16.5 | | |
| | 3* | 0.97 | 29.9 | 17.1 | | |
| SECOR | | 2. | | | | |
| | 5 | 1.74 | | | | |
| | 3 | 2.23 | | | | |
| | 3* | 2.22 | | | | |
| TRANET | | | | | 4.0 | 50.0 |
| Low | 5 | | | | 6.2 | |
| High | 5 | | | | 3.2 | |
| TRANET | | | | | | 0.1 |
| Low | 5 | | | | 6.9 | |
| High | 5 | | | | 3.3 | |
| Camera | ($\alpha$,$\delta$) | | 2. | 2. | | |
| | 3* | | 1.5 | 0.4 | | |

*Pass 3* is a rerun of pass 3, with the addition of data from one plate taken by the collocated PTH-100 camera

Table 4-3
Bias Sigma Resulting from Error Propagation Study

| Laser | Pass | R (m) | A (Sec) | E (Sec) | T (ms) |
|---|---|---|---|---|---|
| | | 0 ± 1. | 0 ± 103 | 0 ± 103 | |
| | 5 | 0.0 ± 1.0 | -49 ± 86 | -30 ± 2 | |
| | 3 | -0.1 ± 1.0 | 181 ± 96 | -24 ± 3 | |
| | 3* | 0.1 ± 1.0 | -1 ± 6 | -18 ± 2 | |
| FPQ-6 | | | | | |
| | | 0 ± 100. | 0 ± 1031 | 0 ± 1031 | 0 ± 50 |
| | 5 | -0.8 ± 1.0 | 14 ± 86 | 29 ± 1 | -0.04 ± 0.05 |
| | 3 | -0.4 ± 1.0 | 257 ± 96 | 13 ± 2 | 0.02 ± 0.08 |
| | 3* | -0.1 ± 1.0 | 74 ± 3 | 19 ± 1 | 0.01 ± 0.08 |
| FPS-16 | | | | | |
| | | 0 ± 100. | 0 ± 1031 | 0 ± 1031 | 0 ± 50 |
| | 5 | 3.7 ± 1.1 | -100 ± 86 | 60 ± 2 | 0.11 ± 0.10 |
| | 3* | 1.5 ± 1.1 | 165 ± 96 | 34 ± 2 | -0.06 ± 0.10 |
| | 3* | 2.8 ± 1.0 | -17 ± 4 | 40 ± 2 | 0.03 ± 0.08 |
| SECOR | | | | | |
| | | 0 ± 100. | | | 0 ± 50 |
| | 5 | -13.3 ± 1.0 | | | -0.98 ± 0.07 |
| | 3 | -6.3 ± 1.1 | | | -1.46 ± 0.12 |
| | 3* | -6.0 ± 1.1 | | | -1.48 ± 0.12 |
| TRANET | | $\dot{R}$ (cm/sec) | | | |
| | | 0 ± 1000. | | | 0 ± 50 |
| Lo | 5 | 17.1 ± 3.3 | | | -1.18 ± 1.17 |
| Hi | 5 | 10.8 ± 3.4 | | | 0.36 ± 1.22 |
| | | 0 ± 1000. | | | 0 ± 0.10 |
| Lo | 5 | 15.0 ± 1.2 | | | -0.00 ± 0.10 |
| Hi | 5 | 11.7 ± 1.2 | | | +0.00 ± 0.10 |
| Camera (Mean) | ($\alpha, \delta$) 3* | | 1.4 | 0.9 | |

*Pass 3* is a rerun of pass 3, with the addition of data from one plate taken by the collocated PTH-100 camera.

SECTION 5

CONCLUSIONS

## 5.1 CONCLUSIONS

With respect to the laser, the systems used in the WICE tests displayed the following consistent biases in the first 10 GEOS-2 passes tracked by the Goddard laser at Wallops Island from April 2 through April 20, 1968.

- SECOR

  R = -10.8 meters

  T = -0.78 millisecond

- FPQ-6

  R = 0.3 meters

  A = 0.25 milliradian, not well determined

  E = 0.13 milliradian

  $T_R$ = 0.37 millisecond

- FPS-16

  R = 2.7 meters

  A = -0.34 milliradian, not well determined

  E = 0.21 milliradian

  $T_R$ = 0.33 millisecond

- TRANET

  Lo $\mathring{R}$ = 17.6 cm/sec

  Hi $\mathring{R}$ = 15.6 cm/sec

  Lo T = was constrained with *a priori* $\sigma_T$ = 0.1 ms

  Hi T = was constrained with *a priori* $\sigma_T$ = 0.1 ms

The consistent SECOR range bias is larger than expected and still not explained. It is not out of the question, however, that the SECOR is correct and the laser incorrect. If this can be shown to be true, it might help explain a similar as yet

unexplained range bias difference observed between this same Goddard laser and the Goddard range and range rate system (GRARR) at Rosman, N. C., when the laser was collocated at the GRARR site in 1966. As yet, there is no explanation for the consistent SECOR time bias although the addition of 0.5 ms to the SECOR time tags in the second and third tapes submitted increased this error.

The C-band radar range biases are smaller than expected. If other C-band radars in the world-wide tracking networks are as accurate as these appear to be, then they are a potential source of large quantities of very accurate and well distributed geodetic data. The elevation angle biases obtained for these radars is consistent with expectations. The timing biases for the two C-band radars agree very well. These should be reduced by about 0.2 ms if the known 0.2 $\pm$ 0.1-ms delay between the Ce clock and the TODG is included in the C-band data.

The unexpectedly large TRANET range rate biases have been explained for the most part. However, this same type of bias apparently affects all the TRANET data in the GSDS, so it is necessary to allow for a bias when doing geodetic calculations with the data.

## SECTION 6
## FUTURE PLANS

### 6.1 FUTURE PLANS

Intercomparisons similar to those given here are planned for the 25 additional laser passes obtained before the WICE tests ended on June 29, 1968. Also, optical data will be added from the cameras collocated with the WICE systems and from many other cameras in the GEOS MOTS and SPEOPT networks in an attempt to further verify these results. Also, simultaneous tracking data from two collocated lasers at Goddard have been collected to help validate the assumption that the laser data are unbiased to within 1 meter.

## APPENDIX A
## GEODETIC SURVEY PROGRAM

### A.1 GENERAL

The geodetic survey was extended from USC&GS first-order triangulation stations EASY, TESTCELL, and ARBUCKLE, using Assateaque Lighthouse as an azimuth check. Intermediate stations named Bridge, and Oboe 2 were established from EASY and TESTCELL at strategic locations that were intervisible with the tracking systems.

The elevation determinations for the tracking systems are in reference to first-order USC&GS benchmarks: G 421 1963, A 299 1949 NACA 3 2 1963 and K 421 1963.

### A.2 COMPUTATIONS

Standard computational procedures were employed to determine the geodetic positions of the antenna systems. All measurements were made to, or reduced to, the centers of rotation of the azimuth circles and the elevation axes of the tracking systems, as specified.

The circuits were analyzed after preliminary computation to determine accuracies. It was found that the closures at ARBUCKLE were all in error in the same direction and to the magnitudes of 11 centimeters in latitude and 7 centimeters in longitude. Circuit closures of the traverse nets performed during this survey revealed excellent ties, the distances being measured with the geodimeter and the angles observed with the Wild T-3 theodolite. Further investigation of the triangulation station ARBUCKLE revealed that it could possibly be disturbed, being located in a cultivated field, even though it is set one foot below the ground level. Also, the recent adjustments applied to the horizontal control in this area by USC&GS may possibly have resulted in slight discrepancies at ARBUCKLE. It was concluded that the most accurate geodetic solution would be obtained by traverse circuits from EASY and TESTCELL, using ARBUCKLE only as a check station.

A.3 CONCLUSIONS

The accuracies of the survey were obtained by the comparison of the angular and distance measurements and the closure on the check station ARBUCKLE. An evaluation of the accuracies is as follows:

| | |
|---|---|
| • Maximum adjustment to the geodimeter distances | 5.55 cms |
| • Average adjustment to geodimeter distances | 1.45 cms |
| • Probable error | 1.45 cms |
| • Average error of geodimeter distances | 1/353,000 |
| • Possible remaining error of geodimeter distances | 1/113,000 |
| • Maximum adjustment to angles | 2.50 sec |
| • Average adjustment to angles | 0.90 sec |
| • Probable error | 0.80 sec |

The average errors in the five positions computed for ARBUCKLE via the five collocation experiment systems nearby and the USC& GS published position were 0.0037 second in latitude and 0.0028 second in longitude. Converting the angular errors to linear errors and determining the resultant, the error is 13.2 centimeters. The ratio error in relation to the distance to EASY is 1:46,300. Therefore, if ARBUCKLE had been used as a tie station, first-order results would have been obtained; but instead, it is felt that higher accuracy was obtained by tying the traverse circuits back at EASY and TESTCELL.

A.4 RESULTS

The following Position and Description of Survey Station sheets list all geodetic information of the tracking systems and the established geodetic survey marks. The information was obtained by reductions of the field data and standard computational procedures.

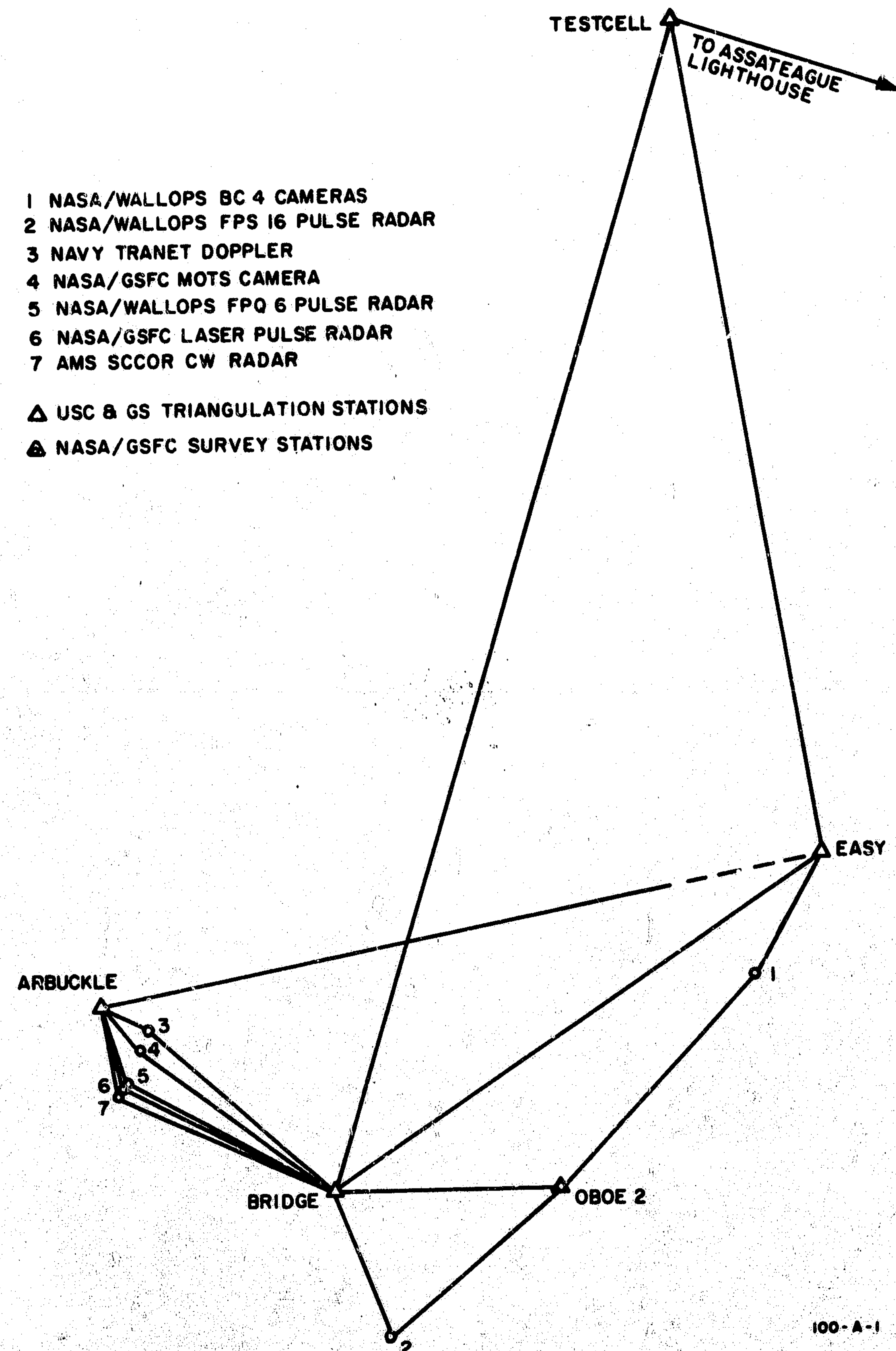


Figure A-1. Geodetic Survey Diagram

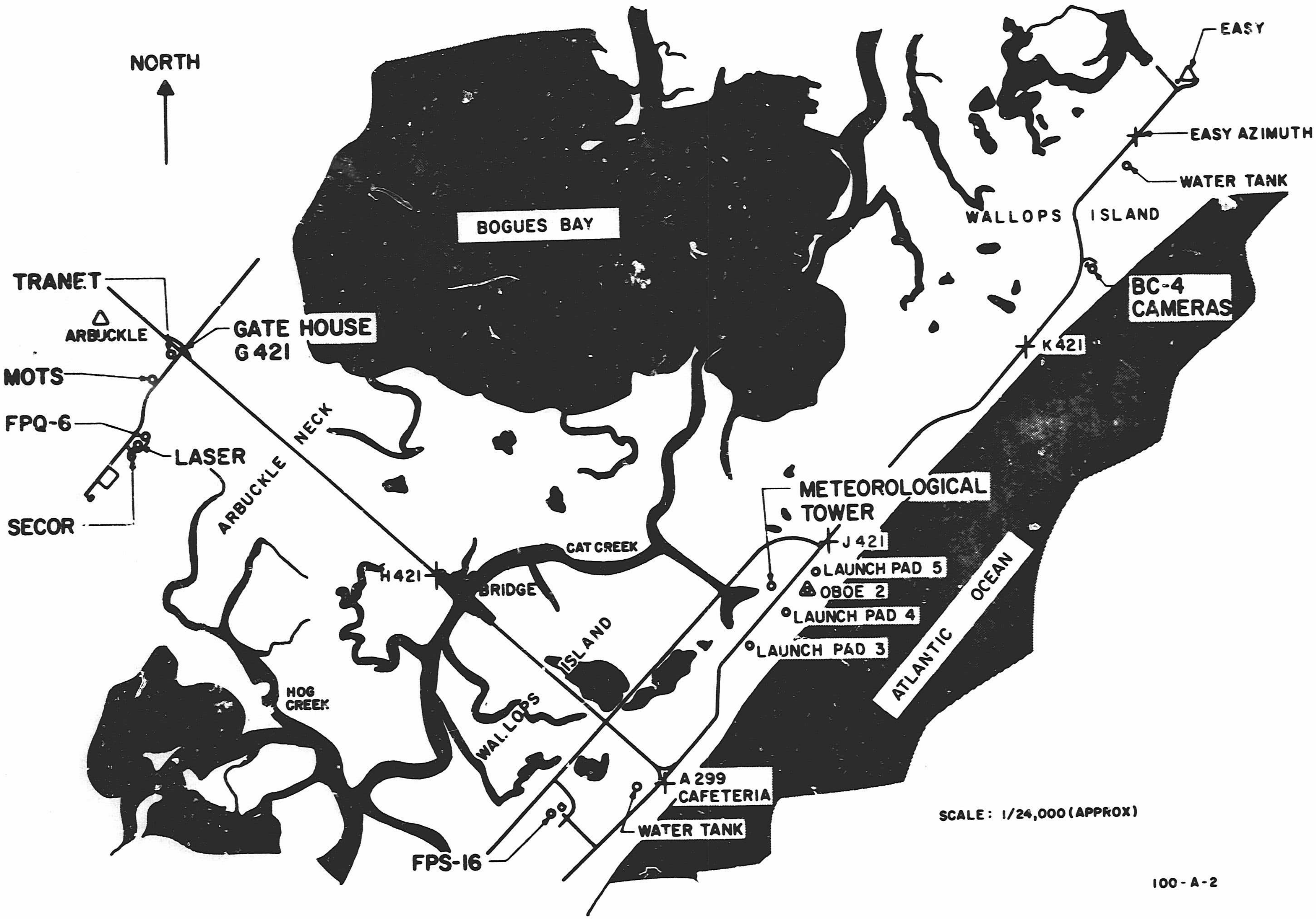


Figure A-2. Layout of Wallops Island Collocation Experiment Systems and Geodetic Control

POSITION AND DESCRIPTION OF SURVEY STATION

| COUNTRY | TYPE OF MARK | STATION | |
|---|---|---|---|
| United States | Brass Tablet | BRIDGE | First Order |
| LOCALITY<br>Wallops Island, Va. | STAMPING ON MARK<br>BRIDGE 1968 | AGENCY (CAST IN MARK)<br>NASA/GSFC | ELEVATION 48.143 FEET<br>14.674 METERS |
| LATITUDE<br>N 37° 51' 07".452 | LONGITUDE<br>W 75° 29' 25".811 | DATUM-ELLIPSOID<br>NAD 1927 Clarke 1866 | ORDER<br>Third |
| LATITUDE | LONGITUDE | DATUM-ELLIPSOID | DATUM<br>SLD 1929 |
| NORTHING | EASTING | GRID AND ZONE | ESTABLISHED BY - AGENCY - DATE<br>NASA/GSFC 3/68 |
| NORTHING | EASTING | GRID AND ZONE | |

TO OBTAIN GRID AZIMUTH, ADD

| OBJECT | (GEODETIC) AZIMUTH | BACK AZIMUTH | GEOD. DISTANCE (M) | GRID DISTANCE (M) (FT) |
|---|---|---|---|---|
| Secor CW Radar | 114-25-06.77 | 294-24-22.42 | 1940.321 | |
| Laser Pulse Radar | 116-28-53.38 | 296-28-09.90 | 1935.018 | |
| FPQ-6 Radar | 117-59-44.75 | 297-59-02.43 | 1908.898 | |
| Walmot # 7078 | 126-25-00.88 | 306-24-19.61 | 2042.731 | |
| TRAJET Doppler | 131-23-36.56 | 311-22-58.04 | 2045.384 | |
| TESTCELL | 197-22-47.15 | 17-24-01.94 | 9955.006 | |
| EASY | 236-40-37.37 | 56-42-19.97 | 4889.117 | |
| Oboe 2 | 270-56-37.42 | 90-57-24.47 | 1874.828 | |
| FPS-16 Radar | 339-43-44.59 | 159-43-55.75 | 1283.715 | |
| Savage Bridge | 353-47-28 | 173-47-28 | 8.641 | |
| | | | | |
| | | | | |
| | | | | |

Station Bridge is located on the highest part of the bridge over Cat Creek leading to Wallops Island, Va. The station is a brass tablet grouted into the walkway on the north side of the bridge. The center is marked by a punch hole at the intersection of an etched cross.

To reach station from the cafeteria at Wallops Island (Bldg. 5005) proceed northwest along blacktop road 0.9 mile to high point in bridge and station.

Savage Bridge was used as a reference mark and is a 1/2-inch metal plug in the eastbound lane of road.

POSITION AND DESCRIPTION OF SURVEY STATION

| COUNTRY | TYPE OF MARK | STATION | |
|---|---|---|---|
| United States | punch hole | Oboe 2 1968 | First Order |
| LOCALITY<br>Wallops Island, Va. | STAMPING ON MARK<br>Oboe 2 1968 | AGENCY (CAST IN MARK)<br>None | ELEVATION 58.561 FEET<br>17.849 METERS |
| LATITUDE<br>N $37^{\circ}$ 51' 06".443 | LONGITUDE<br>W $75^{\circ}$ 28' 09".134 | DATUM–ELLIPSOID<br>NAD 1927 Clarke 1866 | ORDER<br>Third |
| LATITUDE | LONGITUDE | DATUM–ELLIPSOID | DATUM<br>SLD 1929 |
| NORTHING | EASTING | GRID AND ZONE | ESTABLISHED BY – AGENCY – DATE<br>NASA/GSFC 3/68 |
| NORTHING | EASTING | GRID AND ZONE | |

TO OBTAIN GRID AZIMUTH, ADD

| OBJECT | (GEODETIC) AZIMUTH | BACK AZIMUTH | GEOD. DISTANCE (M) | GRID DISTANCE (M) (FT) |
|---|---|---|---|---|
| Bridge | 90-57-24.47 | 270-56-37.42 | 1847.828 | |
| FPS-16 Radar | 50-38-25.03 | 230-37-49.15 | 1849.616 | |
| BC-4 Camera Base | 223-25-41.10 | 43-26-21.67 | 2350.601 | |

Station Oboe 2 is located between launch areas No. 4 and 5 on Wallops Island, Va. The station is a 10-1/2-inch diameter steel plate at the top of a steel inner-tower of a 45-foot wooden outer-tower. The mark is a punch hole at the center of the steel plate.

To reach the station from the cafeteria at Wallops Island (Bldg. 5005) proceed northeast 0.8 mile along blacktop road to a point opposite the tower on the east side of the road.

## POSITION AND DESCRIPTION OF SURVEY STATION

| COUNTRY | TYPE OF MARK | STATION | |
|---|---|---|---|
| United States | Brass Tablet | GEOS RM | First Order |
| LOCALITY: Wallops Island, Va. | STAMPING ON MARK: GEOS RM 1968 | AGENCY (CAST IN MARK): NASA/GSFC | ELEVATION: 18.394 FEET, 5.606 METERS |
| LATITUDE: N 37° 51' 35".107 | LONGITUDE: W 75° 30' 36".216 | DATUM–ELLIPSOID: NAD 1927 Clarke 1866 | ORDER: Third |
| LATITUDE | LONGITUDE | DATUM–ELLIPSOID | DATUM: SLD 1929 |
| NORTHING | EASTING | GRID AND ZONE | ESTABLISHED BY – AGENCY – DATE: NASA/GSFC 3/68 |
| NORTHING | EASTING | GRID AND ZONE | |

TO OBTAIN GRID AZIMUTH, ADD

| OBJECT | (GEODETIC) AZIMUTH | BACK AZIMUTH | GEOD. DISTANCE (M) | GRID DISTANCE (M) (FT) |
|---|---|---|---|---|
| SECOR | 42-01-19.84 | 222-01-18.70 | 68.280 | |
| | | | | |
| Laser | 139-29-00.96 | 312-29-00.69 | 14.870 | |

The GEOS RM station is located at the FPQ-6 C-band facility at the Wallops Island Facility. The station is a brass tablet set in the concrete drive to the front entrance of the FPQ-6 building. The center is marked by a punch hole at the intersection of an etched cross.

To reach from the gate house at the main entrance to Wallops Island facility proceed southwest 0.35 mile to entrance to FPQ-6 C-band facility. The station is located on the southeast edge of the concrete access drive.

POSITION AND DESCRIPTION OF SURVEY STATION

| COUNTRY | TYPE OF MARK | STATION | |
|---|---|---|---|
| United States | punch hole | NASA/Wallops BC-4 Camera Base First Order | |
| LOCALITY: Wallops Island, Va. | STAMPING ON MARK: Wallops BC-4 1968 | AGENCY (CAST IN MARK): | ELEVATION: 26.341 FEET, 8.029 METERS |
| LATITUDE: N 37° 52' 01".807 | LONGITUDE: W 75° 27' 03".023 | DATUM–ELLIPSOID: NAD 1927 Clarke 1866 | ORDER: Third |
| LATITUDE: | LONGITUDE: | DATUM–ELLIPSOID: | DATUM: SLD 1929 |
| NORTHING: | EASTING: | GRID AND ZONE: | ESTABLISHED BY – AGENCY – DATE: NASA/GSFC 3/68 |
| NORTHING: | EASTING: | GRID AND ZONE: | |
| TO OBTAIN | | GRID AZIMUTH, ADD | |

| OBJECT | (GEODETIC) AZIMUTH | BACK AZIMUTH | GEOD. DISTANCE (M) | GRID DISTANCE (M) (FT) |
|---|---|---|---|---|
| EASY | 210-33-10.61 | 30-33-25.57 | 1171.716 | |
| Oboe 2 | 43-26-21.67 | 223-25-41.10 | 2350.601 | |
| BC-4 #273 | 297-13-07.6 | 117-13-07.6 | 0.395 | |
| BC-4 #263 | 97-13-07.6 | 277-13-07.6 | 0.390 | |

BC-4 Camera #273 N 37° 52' 01".802
W 75° 27' 03".009

Elevation of Axis of Rotation 28.216 Feet

BC Camera #263 N 37° 52' 01".809
W 75° 27' 03".039

Elevation of Axis of Rotation 28.216 Feet

Elevation tablet "NAOTS Chincoteague" 9.802 Feet

The BC-4 cameras are located in the northeast area of the NASA Wallops Island facility. The station is a punch hole at the center of circular steel base of the cameras.

To reach station from the cafeteria at Wallops Island (Bldg. 5005) proceed northeast 2.4 miles along blacktop road to the BC-4 camera Dovap Station No. 2 on the east side of the road.

POSITION AND DESCRIPTION OF SURVEY STATION

| COUNTRY | TYPE OF MARK | STATION | |
|---|---|---|---|
| United States | Brass Tablet | AMS SECOR CW Radar First Order | |
| LOCALITY: Wallops Island, Va. | STAMPING ON MARK: Wallops SECOR 1968 | AGENCY (CAST IN MARK): NASA/GSFC | ELEVATION: 27.144 FEET, 8.273 METERS |
| LATITUDE: N 37° 51' 33".462 | LONGITUDE: W 75° 30' 38".086 | DATUM-ELLIPSOID: NAD 1927 Clarke 1866 | ORDER: Third |
| LATITUDE | LONGITUDE | DATUM-ELLIPSOID | DATUM: SLD 1929 |
| NORTHING | EASTING | GRID AND ZONE | ESTABLISHED BY - AGENCY - DATE: NASA/GSFC 3/68 |
| NORTHING | EASTING | GRID AND ZONE | |

TO OBTAIN GRID AZIMUTH, ADD

| OBJECT | (GEODETIC) AZIMUTH | BACK AZIMUTH | GEOD. DISTANCE (M) | GRID DISTANCE (M) (FT) |
|---|---|---|---|---|
| ARBUCKLE | 168-06-20.34 | 348-06-16.39 | 764.353 | |
| Bridge | 294-24-22.42 | 114-25-06.77 | 1940.321 | |
| GEOS RM | 222-01-18.70 | 42-01-19.84 | 68.280 | |

Elevation of Axis of Rotation of Radar 45.833 Feet

The AMS SECOR CW Radar is located near the FPQ-6 facility at the Wallops Island facility. The station is a brass tablet set in the roof of the concrete building centered under the antenna. The center is marked by a punch hole at the intersection of an etched cross.

To reach from the main gate of the Wallops Island facility proceed southwest 0.35 mile along a blacktop road to entrance to station. The station is located on top of small concrete building on the southeast side of road.

GEOS RM was set as a reference mark and is a brass tablet set on the southeast edge of the concrete access drive to the front entrance of the FPQ-6 building.

POSITION AND DESCRIPTION OF SURVEY STATION

| | | | |
|---|---|---|---|
| COUNTRY<br>United States | TYPE OF MARK<br>Support Pipe Center | STATION<br>Navy TRANET Doppler | First Order |
| LOCALITY<br>Wallops Island, Va. | STAMPING ON MARK<br>None | AGENCY (CAST IN MARK)<br>None | ELEVATION<br>44.577 FEET<br>13.587 METERS |
| LATITUDE<br>N 37° 51' 51".314 | LONGITUDE<br>W 75° 30' 28".586 | DATUM–ELLIPSOID<br>NAD 1927 Clarke 1866 | ORDER<br>Third |
| LATITUDE | LONGITUDE | DATUM–ELLIPSOID | DATUM<br>SLD 1929 |
| NORTHING | EASTING | GRID AND ZONE | ESTABLISHED BY – AGENCY – DATE<br>NASA/GSFC 3/68 |
| NORTHING | EASTING | GRID AND ZONE | |

TO OBTAIN GRID AZIMUTH, ADD

| OBJECT | (GEODETIC) AZIMUTH | BACK AZIMUTH | GEOD. DISTANCE (M) | GRID DISTANCE (M) (FT) |
|---|---|---|---|---|
| Bridge | 311-22-58.04 | 131-23-36.56 | 2045.384 | |
| | | | | |
| ARBUCKLE | 116-52-07.79 | 296-51-58.01 | 436.924 | |
| | | | | |
| | | | | |
| | | | | |
| | | | | |
| | | | | |
| | | | | |
| | | | | |
| | | | | |
| | | | | |
| | | | | |

The Navy TRANET Doppler is located at the Information and Observation Building at the main entrance of the Wallops Island facility. The station is on the northwest side of the building at the top of a 45-foot support pipe and at the ground screen level of the antenna array.

POSITION AND DESCRIPTION OF SURVEY STATION

| COUNTRY | TYPE OF MARK | STATION | |
|---|---|---|---|
| United States | Center of Rotation | NASA/GSFC Laser Pulse Radar First Order | |
| LOCALITY: Wallops Island, Va. | STAMPING ON MARK: None | AGENCY (CAST IN MARK): None | ELEVATION: 28.070 FEET / 8.556 METERS |
| LATITUDE: N 37° 51' 35".432 | LONGITUDE: W 75° 30' 36".664 | DATUM-ELLIPSOID: NAD 1927 Clarke 1866 | ORDER: Third |
| LATITUDE | LONGITUDE | DATUM-ELLIPSOID | DATUM: SLD 1929 |
| NORTHING | EASTING | GRID AND ZONE | ESTABLISHED BY - AGENCY - DATE: NASA/GSFC 3/68 |
| NORTHING | EASTING | GRID AND ZONE | |

TO OBTAIN GRID AZIMUTH, ADD

| OBJECT | (GEODETIC) AZIMUTH | BACK AZIMUTH | GEOD. DISTANCE (M) | GRID DISTANCE (M) (FT) |
|---|---|---|---|---|
| ARBUCKLE | 164-22-04.79 | 344-21-59.96 | 713.616 | |
| 300' Meteor. Tower | 283-52-48 | VA + 1° 27' 16" | | |
| Bridge | 296-28-09.90 | 116-28-53.38 | 1935.018 | |
| Water Tank | 306-30-14 | VA + 0° 29' 40" | | |
| 250' Meteor. Tower | 318-13-18 | VA + 1° 13' 29" | | |
| GEOS RM | 312-29-00.69 | 132.29-00.96 | 14.870 | |

The GSFC Laser is located at the FPQ-6 C-band facility at the NASA Wallops Island facility. The station is the centers of rotation of the azimuth and elevation axes of the Laser.

To reach the station from the gate house at the main entrance to the Wallops Island facility proceed southwest 0.35 mile to entrance FPQ-6 C-band facility. The Laser is located on the concrete apron at the southwest side of the building.

Slant Range to near surface of water tank at guard rail height 3274.977 meters.

POSITION AND DESCRIPTION OF SURVEY STATION

| COUNTRY | TYPE OF MARK | STATION | |
|---|---|---|---|
| United States | Brass Tablet | NASA/GSFC MOTS Camera First Order | |
| LOCALITY: Wallops Island, Va. | STAMPING ON MARK: WALMOT NO 7078 1968 | AGENCY (CAST IN MARK): NASA/GSFC | ELEVATION: 22.728 FEET, 6.927 METERS |
| LATITUDE: N 37° 51' 46".779 | LONGITUDE: W 75° 30' 33".060 | DATUM-ELLIPSOID: NAD 1927 Clarke 1866 | ORDER: Third |
| LATITUDE | LONGITUDE | DATUM-ELLIPSOID | DATUM: SLD 1929 |
| NORTHING | EASTING | GRID AND ZONE | ESTABLISHED BY - AGENCY - DATE: NASA/GSFC 3/68 |
| NORTHING | EASTING | GRID AND ZONE | |

TO OBTAIN GRID AZIMUTH, ADD

| OBJECT | (GEODETIC) AZIMUTH | BACK AZIMUTH | GEOD. DISTANCE (M) | GRID DISTANCE (M) (FT) |
|---|---|---|---|---|
| Bridge | 306-24-19.61 | 126-25-00.88 | 2042.731 | |
| | | | | |
| ARBUCKLE | 140-16-13.46 | 320-16-06.42 | 438.668 | |

Elevation of Axis of Rotation of Camera 24.798 Feet

The GSFC MOTS camera is located near the main entrance of the Wallops Island facility. The station is a brass tablet set in the center of the concrete pier of the camera base. The center is marked by a punch hole at the intersection of an etched cross.

To reach from the main gate of the Wallops Island facility proceed southwest 0.1 mile along blacktop road to station on northwest side of road.

POSITION AND DESCRIPTION OF SURVEY STATION

| COUNTRY | TYPE OF MARK | STATION | |
|---|---|---|---|
| United States | Cente · of Rotation | NASA/Wallops FPQ-6 Pulse Radar First Order | |
| LOCALITY<br>Wallops Island, Va. | STAMPING ON MARK<br>None | AGENCY (CAST IN MARK)<br>None | ELEVATION<br>49.060 FEET<br>14.953 METERS |
| LATITUDE<br>N 37° 51' 36".509 | LONGITUDE<br>W 75° 30' 34".764 | DATUM-ELLIPSOID<br>NAD 1927 Clarke 1866 | ORDER<br>Third |
| LATITUDE | LONGITUDE | DATUM-ELLIPSOID | DATUM<br>SLD 1929 |
| NORTHING | EASTING | GRID AND ZONE | ESTABLISHED BY - AGENCY - DATE<br>NASA/GSFC 3/68 |
| NORTHING | EASTING | GRID AND ZONE | |
| TO OBTAIN | | GRID AZIMUTH, ADD | |

| OBJECT | (GEODETIC) AZIMUTH | BACK AZIMUTH | GEOD. DISTANCE (M) | GRID DISTANCE (M) (FT) |
|---|---|---|---|---|
| Bridge | 297-59-02.43 | 117-59-44.75 | 1908.898 | |
| | | | | |
| ARBUCKLE | 159-56-42.39 | 339-56-36.39 | 696.220 | |

NASA/Wallope FPQ-6 Pulse Radar is located at the FPQ-6 facility of the NASA Wallops Island, Va. facility. The station is the centers of rotation of the azimuth and elevation axes of the antenna.

To reach from the main gate of the Wallops Island facility proceed southwest 0.35 mile along blacktop road to the entrance to the FPQ-6 facility on the southeast side of the road. The antenna is located at the northeast end of the FPQ-6 operations building.

POSITION AND DESCRIPTION OF SURVEY STATION

| COUNTRY | TYPE OF MARK | STATION | |
|---|---|---|---|
| United States | Center of Rotation | NASA/Wallops FPS-16 Pulse Radar First Orde | |
| LOCALITY: Wallops Island, Va. | STAMPING ON MARK: None | AGENCY (CAST IN MARK): None | ELEVATION: 40.658 FEET, 12.393 METERS |
| LATITUDE: N 37° 50' 28".393 | LONGITUDE: W 75° 29' 07".622 | DATUM-ELLIPSOID: NAD 1927 Clarke 1866 | ORDER: Third |
| LATITUDE | LONGITUDE | DATUM-ELLIPSOID | DATUM: SLD 1929 |
| NORTHING | EASTING | GRID AND ZONE | ESTABLISHED BY - AGENCY - DATE: NASA/GSFC 3/68 |
| NORTHING | EASTING | GRID AND ZONE | |

TO OBTAIN GRID AZIMUTH, ADD

| OBJECT | (GEODETIC) AZIMUTH | BACK AZIMUTH | GEOD. DISTANCE (M) | GRID DISTANCE (M) (FT) |
|---|---|---|---|---|
| Bridge | 159-43-55.75 | 339-43-44.59 | 1283.715 | |
| Oboe 2 | 230-37-49.15 | 50-38-25.03 | 1849.616 | |

The FPS-16 Pulse Radar is located at the AN/FPS-16 Radar facility at Wallops Island, Va. The station is the centers of rotation of the azimuth and elevation axes of the radar antenna.

To reach from the cafeteria at the Wallops Island (Bldg. 5005) proceed southwest 0.3 mile along blacktop road to entrance to FPS-16 facility, then proceed northwest 0.2 mile to station. The radar antenna is located on the roof of and at the southwest corner of the FPS-16 Operations Building.

## APPENDIX B
## WICE C-BAND PREPROCESSOP PROGRAM

### B.1 DATA PREPROCESSING

Data are processed in the following manner: Sum and average the pre- and postcalibration functions.

| | I. D. Number | | Function |
|---|---|---|---|
| | Precal | Postcal | |
| a. | 101-122 | 201-222 | AGC step cal. |
| b. | 123 | 223 | Boresight normal (A, E) |
| c. | 124 | 224 | Boresight plunge (A, E) |
| d. | 125 | 225 | Range target skin (R) |
| e. | 126 | 226 | Range target beacon (R) |
| f. | 140 | 240 | Doppler, CSP + 1 line ($\mathring{R}$) |
| g. | 141 | 241 | Doppler, CSP - 1 line ($\mathring{R}$) |

Process data, selecting every Nth point with the following corrections applied:

a. Time tag correction:

$$t_c = t_o + R/C \qquad c = \text{velocity of light}$$

b. The data are interpolated to the even second, utilizing Newton's interpolation formula with divided differences.

c. Refraction: Refraction is always applied. If input information is not available, the following nominal values are used:

$$\mu - 1 = 0.2919 \text{ X } 10^{-3}$$

Value for scale height is also built-in

$$S = 7600 \text{ meters}$$

Elevation Refraction:

$$E_c = E_o - \text{Cot } (E_o) \cdot (\mu - 1.)$$

Range Refraction:

$$R_c = R_o - (\mu-1) \cdot S/\sin E_c$$

The data can be merged with a previously generated GDAP format data tape.

Input Data Format

(12, 1X, 12, 1X, A8, 1X, 6E10.0)

The data are organized in group (NGRP) and sets (NSET) to facilitate data handling. Card arrangement for the data is:

| | | | | | |
|---|---|---|---|---|---|
| NGRP | NSET | LABEL | DATA(1) | DATE(2), --- | DATA(6) |
| 12, 1X, | 12, 1X, | A8, 1 X, | E10.0 | E10.0 --- | E10.0 |

NGRP = 1, NSET = 1

DATA (1) - 113 – Designator for C-BAND DATA

DATA (2) - XX.00 MINIMUM SEPARATION BETWEEN DATA POINTS (sec)

NGRP = 2 NSET = 1

DATA (1) XX. Station Number

(2) YRMODY. Universal data of observation yr, mo, day

(3) YRMODY. Data of Reduction, yr, mo, day

(4) XXXX. Orbit Number

(5) 0. First pass computes measurement and output is on Tape 2

1. Computes the measurement and merges data with the previously written tape.

Input - Unit 1

Output - Unit 2

NGRP = 3 NSET = 1

| | | |
|---|---|---|
| DATA (1) | HH. | Start hour of day of observation |
| (2) | MM. | Start minute of day of observation |
| (3) | SS. | Start second of day of observation |
| (4) | HH. | Stop hour of day of observation |
| (5) | MM. | Stop minute of day of observation |
| (6) | SS. | Stop second of day of observation |

NGRP = 4 NSET = 1

| | | |
|---|---|---|
| DATA (1) | 0. | Do not save input tape on unit 1 |
| | 1. | Save input tape on unit 1 |

NGRP = 5 NSET = 1

| | | |
|---|---|---|
| DATA (1) | XXXX.XXX | Total atmospheric pressure (MM Mercury) |
| (2) | XXXX.XXX | Partial pressure of water vapor (MM Mercury) |
| (3) | XXXX.XXX | Absolute Temperature (c) |

NGRP = 6 NSET = 1

| | | |
|---|---|---|
| DATA (1) | XXXXX.XXX | Conversion factor for range and range-rate for feet to meters = 0.3048 |
| (2) | XXXXX.XXX | Scale multiplier for range rate to correct current error in magnitude of $10^8$ in range rate |
| (3) | XX.0 | = 0.0 use interpolation scheme to the even second |
| | | = 1.0 utilize data as acquired from tape |

(4) XXXX.XXX Maximum time (seconds after $0^h$ UTC). Larger than any data time tag in pass. Needed for program to pass over gaps in data span.

NOTE

The values for NGRP 6 are preset to 1.0, 1.0, 0.0, 0.0, respectively. If NGRP 6 card is input, then new values have to be given for each one.

NOTE

The feature for printing of a word position summary as in GPRO is also a part of C-BAND. Load the GROUP 1 card for all previous systems prior to C-BAND data cards.

## REFERENCES


1. Moss, S. J. and Wells, W. T.,"An Analysis of the GSFC Laser Ranging Data", submitted to Goddard Space Flight Center in fulfillment of Contract NAS5-9756-42, June 16, 1967.

2. Gross, J. W. III,"Preprocessing Electronic Satellite Observations", prepared for National Aeronautics and Space Administraction, Contract No. NGR 36-008-093, OSURF Project No. 2514, March 1968.

3. "Tranet Station Operation Manual (Tran SOM)", prepared by the John Hopkins University Applied Physics Laboratory, Contract NOw6Z-0604-C, Document TG-424A.

4. "Final Report Measurements and Analysis Performance of MIPIR, Missile Precision Instrumentation Radar Set AN/FPQ-6", contract NOw61-0428d. Prepared by Radio Corporation of America, M. and S.R., Moorestown, New Jersey, December 1964.

5. Berbert, J. H., Reich, R., Maresca, P., Norris, P., "Intercomparison of Collocated Laser Optical and GRARR Radio Ranging System Tracks on GEOS-A" GSFC Document X-514-67-447, September 1967.

6. Stanley, H. R. "Calibration and Evaluation of AN/FPQ-6 Radar Utilizing GEOS-11 Satellite, A Status Report" NASA Wallops Station Document X-16-68-1, August 1968.

7. Berbert, J. H., "Intercomparison of GEOS-A Observation Systems, "GSFC Document X-514-67-315, July 1967.

8. J. G. Hartwell, "Variations in the Mathematical Modeling for GEOS-A" Proceedings of the GEOS Program Review Meeting 12-14 December 1967.

9. F. J. Lerch et. al. "GEOS-1 Station Tracking Positions on the SAO Standard Earth (C-5)" GSFC Document X-552-68-70 December 1967.

10. F.J. Lerch et. al. "Gravity Model Comparison using GEOS-1 Long Arc. Orbital Solutions". GSFC Document X-552-68-71, December 1967.